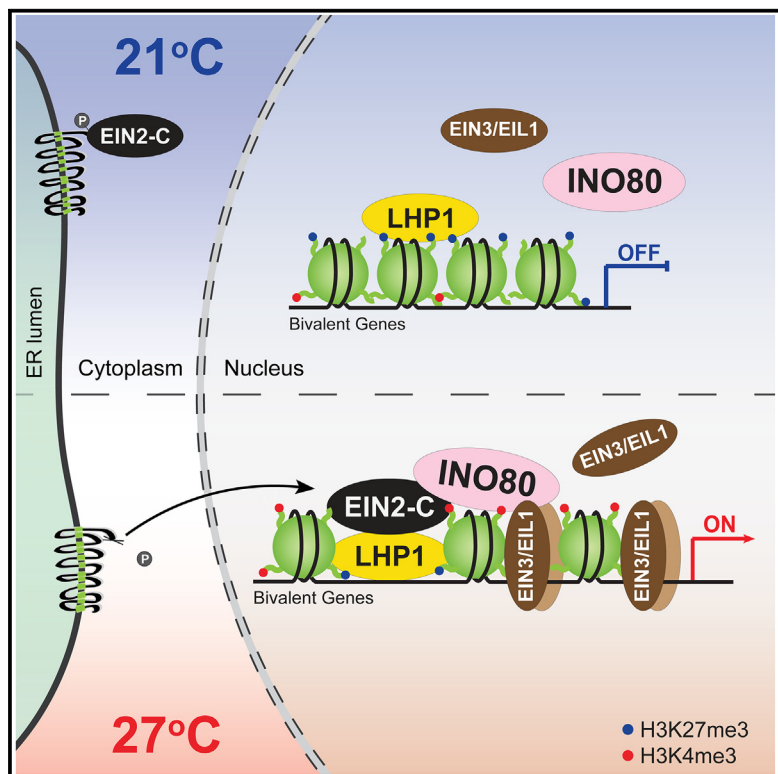


LHP1 and INO80 cooperate with ethylene signaling for warm ambient temperature response by activating specific bivalent genes

Graphical abstract



Authors

Zhengyao Shao, Yanan Bai, Enamul Huq,
Hong Qiao

Correspondence

hqiao@austin.utexas.edu

In brief

Shao et al. demonstrate that increased ambient temperature induces ethylene signaling. The ethylene signaling key factors EIN2 and EIN3 collaborate with LHP1 and INO80 to orchestrate chromatin bivalency switching by depositing H3K4me3 and depleting H3K27me3, enabling rapid transcriptional activation in response to elevated temperatures.

Highlights

- Warm temperature triggers ethylene signaling
- EIN2 and EIN3 work with LHP1 and INO80 to switch chromatin bivalency in warm temperature
- EIN2-LHP1-INO80-EIN3 module deposits H3K4me3 and depletes H3K27me3 in warm temperature
- Chromatin bivalency switching in warm temperature alters target gene expression



Article

LHP1 and INO80 cooperate with ethylene signaling for warm ambient temperature response by activating specific bivalent genes

Zhengyao Shao,^{1,2} Yanan Bai,^{1,2} Enamul Huq,^{1,2} and Hong Qiao^{1,2,3,*}¹Institute for Cellular and Molecular Biology, The University of Texas at Austin, Austin, TX 78712, USA²Department of Molecular Biosciences, The University of Texas at Austin, Austin, TX 78712, USA³Lead contact*Correspondence: hqiao@austin.utexas.edu<https://doi.org/10.1016/j.celrep.2024.114758>

SUMMARY

Ethylene signaling has been indicated as a potential positive regulator of plant warm ambient temperature response, but its underlying molecular mechanisms are largely unknown. Here, we show that LHP1 and INO80 cooperate with ethylene signaling for warm ambient temperature response by activating specific bivalent genes. We found that the presence of warm ambient temperature activates ethylene signaling through EIN2 and EIN3, leading to an interaction between LHP1 and accumulated EIN2-C to co-regulate a subset of LHP1-bound genes marked by H3K27me3 and H3K4me3 bivalency. Furthermore, we demonstrate that INO80 is recruited to bivalent genes by interacting with EIN2-C and EIN3, promoting H3K4me3 enrichment and facilitating transcriptional activation in response to a warm ambient temperature. Together, our findings illustrate a mechanism wherein ethylene signaling orchestrates LHP1 and INO80 to regulate warm ambient temperature response by activating specific bivalent genes in *Arabidopsis*.

INTRODUCTION

As sessile organisms, plants need to adapt to the ever-changing environments and rapidly respond to various abiotic and biotic stresses for optimal growth and survival. Over the past few decades, global warming resulting in a gradual increase in temperature has placed significant challenges on plant growth, development, and, more importantly, crop yield.^{1,2} When exposed to an increased ambient temperature, plants alter both their both above-ground and below-ground architectures, termed thermomorphogenesis, which involves various phenotypic changes, such as elongated hypocotyl, root, petiole, and early flowering, to cope with warm ambient temperature stress through a series of molecular mechanisms, including transcriptional and translational regulations.^{3–5} Initially, the warm ambient temperature signal is perceived by plant thermosensors, such as phytochrome B (phyB) and a prion-like domain in EARLY FLOWERING 3 (ELF3).^{6–9} Following warm ambient temperature signal transduction, the PHYTOCHROME INTERACTING FACTOR 4 (PIF4), a basic-helix-loop-helix transcription factor (TF) playing important roles in the light signaling pathway, serves as the master regulator to facilitate most of the downstream transcriptional responses, including hypocotyl elongation and early flowering.^{10–12} Specifically, accumulated PIF4 under a warm ambient temperature condition directly activates the transcription of both auxin biosynthesis genes and auxin signaling and response genes, such as INDOLE-3-ACETIC ACID (IAA) and SMALL AUXIN UP RNA (SAUR) families. This process leads to an in-

crease in auxin content and the activation of auxin signal transduction, promoting hypocotyl elongation under a warm ambient temperature.^{11,13,14} Recent studies have showcased ethylene signaling as a potential positive regulator of warm ambient temperatures.¹⁵ Mutations in ethylene receptor ETHYLENE RESPONSE 1 (ETR1) and key factors in ethylene signal transduction pathway ETHYLENE INSENSITIVE 2 (EIN2) and EIN3 result in a decreased thermotolerance; in contrast, a constitutive ethylene responsive mutant of CONSTITUTIVE TRIPLE RESPONSE 1 (CTR1) is more tolerant to heat shock treatment.^{16,17} HEAT SHOCK TRANSCRIPTION FACTOR A7 (HSFA7a) and HSFA7b are reported to regulate both ethylene signaling and ethylene biosynthesis homeostasis to properly establish thermotolerance and thermopriming at shoot apical meristem tissues.¹⁸ Moreover, a recent study showed that EIN3 protein is stabilized by warm ambient temperature (27°C) due to the degradation of its negative regulators EIN3-binding F box protein 1 (EBF1) and EBF2 by salt- and drought-induced ring finger 1 (SDR1).¹⁹ These studies strongly suggest that ethylene signaling potentially functions as a positive regulator of the warm ambient temperature response. However, the molecular mechanisms underlying the involvement of ethylene signaling in the warm ambient temperature response largely remain to be investigated.

Environmental stimuli have been shown to cause changes in epigenetic landscapes, especially for histone modifications in *Arabidopsis*.^{20–22} For instance, when challenged with a warm ambient temperature, H2A.Z-containing nucleosomes evict



H2A.Z to regulate global transcriptome in an INOSITOL AUXOTROPHY 80 (INO80) chromatin-remodeling-complex-dependent manner.^{23,24} HISTONE DEACETYLASE 9 (HDA9) also facilitates the warm-ambient-temperature-responsive H2A.Z depletion at the *YUCCA8* (*YUC8*) gene locus to promote PIF4 DNA binding to its promoter.^{25,26} VERNALIZATION INSENSITIVE 3-LIKE 1 (VIL1), the facultative component of Polycomb repressive complex 2 (PRC2), regulates both chromatin looping in concert with phyB to promote plant growth in response to temperature fluctuation and global H3K27me3 enrichment under warm ambient temperature conditions to accelerate the flowering process.^{27,28} The H3K4me3 demethylases JUMONJI DOMAIN-CONTAINING PROTEINS 14 and 15 (JMJ14/15) erase H3K4me3 marks at gene loci of the negative regulator of the warm ambient temperature response and repress their gene expressions to ensure a proper thermosensory response, while RELATIVE OF EARLY FLOWERING 6 (REF6)/JMJD12 demethylates H3K27me3 at gene loci of the positive regulator of thermomorphogenesis to promote their active gene expression.^{29,30} Therefore, by altering histone modifications in response to environmental cues, epigenetic modifications play an essential role in regulating gene expression to modulate plant development, growth, and adaptation to changing environmental conditions.

In this study, we found that LHP1 and INO80 cooperate with ethylene signaling for warm ambient temperature response by activating specific bivalent genes. We found that the ethylene-insensitive mutants *ein2-5* and *ein3-1 eil1-1* and the PRC component *LIKE HETEROCHROMATIN PROTEIN 1* (*LHP1*) loss-of-function *lhp1-3* mutant displayed a partially impaired warm ambient temperature response. Further transcriptomic analysis showed that *ein2-5*, *ein3-1 eil1-1*, and *lhp1-3* have a similar reduced response to warm ambient temperatures at a molecular level. Moreover, our result demonstrated that warm ambient temperature triggers ethylene signaling, leading to the accumulation of EIN2 C terminus (EIN2-C) and EIN3 proteins. This accumulation results in an enhanced interaction between LHP1 and EIN2-C, targeting a subset of warm-ambient-temperature-responsive bivalent genes marked by both H3K27me3 and H3K4me3. Furthermore, we found that INO80 is recruited to these bivalent genes through its interaction with EIN2-C and EIN3, facilitating the enrichment of H3K4me3 to counteract the repressive function of H3K27me3 for a rapid transcription activation in response to warm ambient temperatures. In summary, our findings reveal a mechanism wherein ethylene signaling orchestrates LHP1 and INO80 to regulate the warm ambient temperature response by activating specific bivalent genes in *Arabidopsis*.

RESULTS

EIN2, EIN3, and LHP1 participate in warm ambient temperature response

During our study of ethylene and temperature responses, we found that warm-ambient-temperature (27°C)-induced elongation in hypocotyl in Col-0 was reduced in the key ethylene signaling component mutants *ein2-5* and *ein3-1 eil1-1* (Figures S1A and S1B). The reduction was also observed in *lhp1-3*, the null mutant of a PRC component, *LHP1*

(Figures S1A and S1B).³¹ To further investigate how ethylene and LHP1 are involved in the warm ambient temperature response, we conducted histochemical staining for β-glucuronidase (GUS) activity of ethylene reporter 5xEBS::GUS in response to a warm ambient temperature.³² The result showed that warm ambient temperature leads to an elevation of ethylene signaling (Figure S1C). We then examined EIN2, EIN3, and LHP1 protein levels under a warm ambient temperature (27°C) treatment. EIN2 cleavage and EIN3 protein accumulation were induced by a warm ambient temperature (Figures S1D and S1E). However, the level of LHP1 protein remains unchanged (Figure S1F).

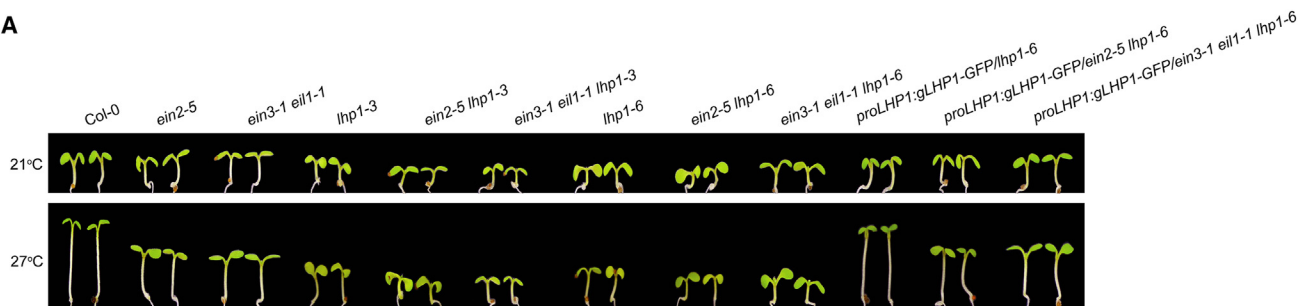
Next, we compared the transcriptomes of Col-0, *ein2-5*, *ein3-1 eil1-1*, and *lhp1-3* with or without 4 h of 27°C treatment (Figures S1G and S1H). We found that warm-ambient-temperature-induced transcriptional activation in Col-0 was compromised in the *ein2-5*, *ein3-1 eil1-1*, and *lhp1-3* mutants with a similar expression pattern (Figures S1G and S1H). Subsequent statistical analysis further confirmed that the reduction was significant in all three mutants compared to Col-0 (Figure S1H). More importantly, the reductions observed in *ein2-5*, *ein3-1 eil1-1*, and *lhp1-3* were statistically comparable, suggesting the potential co-functionality of EIN2, EIN3, and LHP1 in response to a warm ambient temperature.

EIN2 interacts with LHP1 to regulate warm ambient temperature response

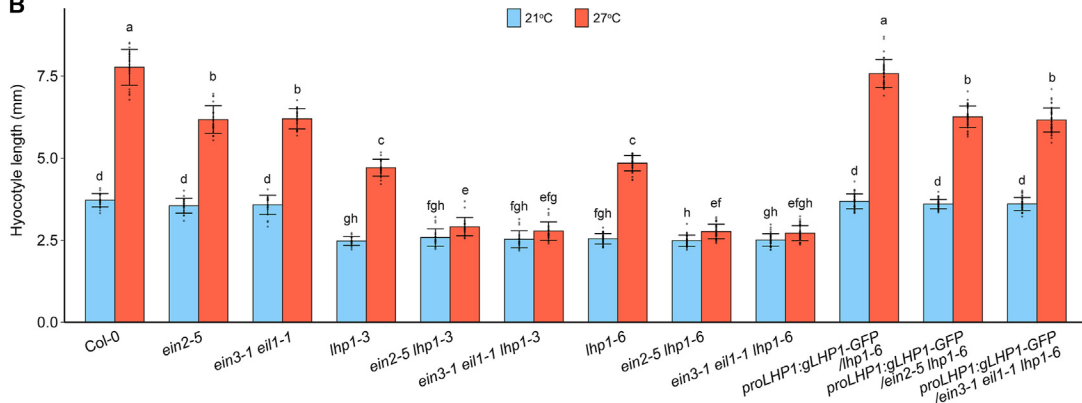
To investigate the relationship between LPH1 and EIN2 or EIN3 in the context of a warm ambient temperature response, we first generated *ein2-5 lhp1-3* and *ein2-5 lhp1-6* double mutants and *ein3-1 eil1-1 lhp1-3* and *ein3-1 eil1-1 lhp1-6* triple mutants. A warm ambient temperature response assay showed a significant reduction in warm-ambient-temperature-induced hypocotyl elongation in *ein2-5 lhp1-3* and *ein2-5 lhp1-6* double mutants, as well as *ein3-1 eil1-1 lhp1-3* and *ein3-1 eil1-1 lhp1-6* triple mutants, compared to the *ein2-5* and *lhp1-3* or the *ein3-1 eil1-1* mutants, respectively (Figures 1A and 1B). Notably, these higher-order mutants exhibited almost no response to a warm ambient temperature (Figures 1A and 1B). Our further test with PIF4, the master regulator of thermomorphogenesis, protein levels showed that in *ein2-5*, *ein3-1 eil1-1*, and *lhp1-3*, as well as in *ein2-5 lhp1-3* and *ein3-1 eil1-1 lhp1-3*, PIF4 protein is accumulated to the same level as in Col-0 under warm ambient temperature treatment, suggesting that the initial warm ambient temperature response by PIF4 accumulation is not impaired in these single mutants nor higher-order mutants (Figures S2A and S2B).^{3,14} To further validate the additive genetic function of LHP1 with EIN2 and EIN3 in the warm ambient temperature response, we introduced *proLHP1::gLHP1-GFP* into *lhp1-6*, *ein2-5 lhp1-6*, and *ein3-1 eil1-1 lhp1-6* mutants and examined their responses to warm ambient temperatures.³³ The phenotypes of *lhp1-6*, *ein2-5 lhp1-6*, and *ein3-1 eil1-1 lhp1-6* were restored by *proLHP1::gLHP1-GFP* to that of Col-0, *ein2-5*, or *ein3-1 eil1-1*, respectively (Figures 1A, 1B, and S2C), further confirming that LHP1 functions with EIN2 and EIN3/EIL1 additively in response to a warm ambient temperature.

To understand the molecular basis of the synergistic function of EIN2, EIN3, and LHP1, we performed yeast two-hybrid (Y2H) assays and found that EIN2-C, rather than EIN3, could interact

A



B



C

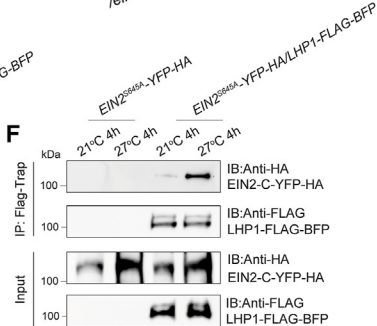
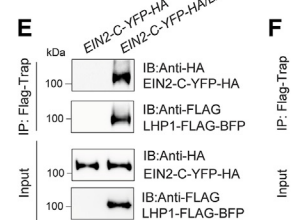
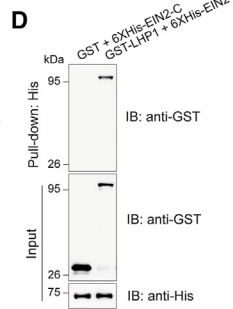
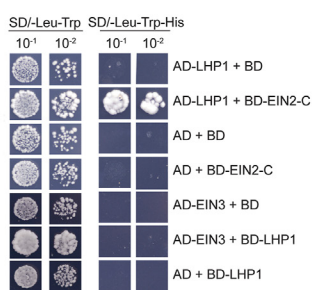


Figure 1. EIN2 associates with LHP1 to regulate the warm ambient temperature response

(A) Representative images of seedlings of indicated plants grown on Murashige and Skoog (MS) medium at either 21°C or 27°C.

(B) Measurements of hypocotyl lengths of indicated plants in (A). Values are means ± SD of at least 30 seedlings. Different letters represent significant differences between each genotype calculated by a one-way ANOVA test followed by Tukey's honestly significant difference (HSD) test with $p \leq 0.05$.

(C) Y2H assays to detect the interaction between LHP1 and EIN2-C or EIN3. BD, GAL4 DNA binding domain; AD, GAL4 activation domain. LHP1 was fused to AD and used as a bait protein to test the interaction between EIN2-C and LHP1; AD-EIN3 was used as a bait protein to test the interaction between EIN3 and LHP1. Left: yeasts grown on two-dropout medium (SD/-Leu-Trp) served as a loading control. Right: yeast grown on selective three-dropout medium (SD/-Leu-His-Trp) as an experiment group.

(D) *In vitro* pull-down experiment to validate the interaction between LHP1 and EIN2-C. 6xHis-tagged EIN2-C and GST-tagged LHP1 were purified from *E. coli* and subjected to pull-down experiments. GST was used as a negative control.

(E) Pull-down assays of EIN2-C (EIN2-C-YFP-HA) with LHP1 (LHP1-FLAG-BFP) in tobacco. The total proteins from the tobacco leaves co-transformed with EIN2-C-YFP-HA and LHP1-FLAG-BFP were applied to the IP by FLAG-Trap magnetic agarose (DYKDDDDK Fab-Trap) using LHP1-FLAG-BFP as bait. The pull-down products were detected in immunoblots against anti-HA antibody or anti-FLAG antibody. IP using protein extracts from tobacco leaves expressing EIN2-C-YFP-HA alone serves as a negative control.

(F) *In vivo* coIP assay to examine the interaction between EIN2-C and LHP1. Five-day-old LHP1-FLAG-BFP/EIN2^{S645A}-YFP-HA transgenic green seedlings treated with or without 4 h of 27°C were subjected to IP with FLAG-Trap magnetic agarose (DYKDDDDK Fab-Trap); IP in EIN2^{S645A}-YFP-HA transgenic green seedlings serves as a negative control. Anti-HA antibody or anti-FLAG antibody was used to detect IP products. IB, immunoblotting; IP, immunoprecipitation. See also Figures S1 and S2A-S2D.

with LHP1 (Figures 1C and S2D). The following *in vitro* pull-down assays using proteins expressed in *E. coli* and tobacco leaves validated the direct physical interaction between EIN2-C and

LHP1 (Figures 1D and 1E). To further confirm the interaction between LHP1 and EIN2-C *in vivo* under the warm ambient temperature condition, we performed a co-immunoprecipitation (coIP)

assay in the *LHP1-FLAG-BFP/EIN2^{S645A}-YFP-HA* plants with or without 4 h of 27°C treatment (Figure 1F). An increased interaction between EIN2-C and LHP1 was detected when 35S::*LHP1-FLAG-BFP/EIN2^{S645A}-YFP-HA* transgenic plants were treated with 27°C for 4 h (Figure 1F). These results provide an additional piece of biochemical evidence that LHP1 and EIN2 function collaboratively in responses to a warm ambient temperature.

EIN2, EIN3, and LHP1 target common genes for transcriptional activation at warm ambient temperature

To further investigate the collective function of EIN2 and LHP1 in the warm ambient temperature response, we performed mRNA sequencing (mRNA-seq) of *ein2-5 lhp1-3* and compared the warm-ambient-temperature-activated differentially expressed genes (DEGs) in *ein2-5 lhp1-3* with those in *ein2-5* and *lhp1-3* single mutants and Col-0 (Figure S2E). We found that 205 of the DEGs were both EIN2 and LHP1 dependent, as their log₂ fold change (log₂FC) value is the lowest in *ein2-5 lhp1-3* compared with those in *ein2-5*, *lhp1-3*, and Col-0 (Figure 2A). Gene Ontology (GO) analysis showed that the biological processes of response to heat, response to stimulus, and cellular response to stimulus were significantly enriched (Figure S2F). We also found numbers of well-studied growth-promoting and stress-responsive genes within this EIN2-LHP1-dependent warm-ambient-temperature-induced DEG category (Figure 2B).

The genetic interaction between EIN3 and LHP1 and the phenotypic similarity between *ein3-1 eil1-1 lhp1-3* and *ein2-5 lhp1-3* prompted us to investigate how EIN3 is involved in EIN2-LHP1-dependent warm-ambient-temperature-induced transcriptional activation. We searched for the EIN3 binding motifs in the upstream 2,000 bp (~2 kb) from the start codon (ATG) in 205 of EIN2-LHP1-dependent DEGs using the *de novo* EIN3 binding motif (A/T)(T/C)G(A/C/T)A(T/C/G)(C/G)T(T/G).³⁴ 124/205 of EIN2-LHP1-dependent ambient-temperature-activated DEGs have at least one putative EIN3 binding motif (Figure 2C). Notably, the reduction in transcriptional activation of 124 genes with EIN3 binding motif(s) was more significant than that of the genes without an EIN3 binding motif in *ein2-5 lhp1-3* (Figure 2C). Our RT-qPCR assay of four representative target genes, *BIM1*, *BUD2*, *GA3ox1*, and *SAUR76*,^{35–38} in different genetic backgrounds further confirmed that EIN3 is required for their transcriptional activation in response to warm ambient temperatures (Figures S3 and S4A–S4D). Importantly, the decrease in warm-ambient-temperature-induced transcriptional activation resulting from *EIN3/EIL1* mutations was also found in the *ein3-1 eil1-1 lhp1-3* triple mutants, which is similar to that observed in the *ein2-5 lhp1-3* double mutant (Figures 2C and S3). This implies that EIN3 plays a role in the EIN2-LHP1-dependent warm ambient temperature response.

Considering that EIN3 binding motifs have been identified *in silico* within the promoter regions of EIN2-LHP1-dependent DEGs, and EIN3 is required for their transcription activation in response to a warm ambient temperature (Figures 2C, S3, and S4A–S4D), we examined EIN3 binding to those target genes in response to a warm ambient temperature. Chromatin IP (ChIP)-qPCR assay results showed that EIN3 binding was highly enriched when Col-0 seedlings were subject to warm ambient temperature treatment (Figures 2D–2G and S4A–S4H). More-

over, the elevated EIN3 binding by a warm ambient temperature was significantly reduced in the *lhp1-3* mutant, although there is no significant difference in the endogenous EIN3 levels between Col-0 and *lhp1-3* (Figures 2D–2G and S4I).

As LHP enhances EIN3's function in the warm ambient temperature response, and LHP1 can associate with chromatin, we therefore analyzed a published LHP1 ChIP-seq dataset.³⁹ The LHP1 binding enrichment was detected in our target genes, and more importantly, there is a noteworthy preference for LHP1 binding in EIN2-LHP1-dependent DEGs compared to the entire *Arabidopsis* genome (Figures S4J–S4N). Subsequent ChIP-qPCR over selected target genes in *proLHP1::gLHP1-GFP/lhp1-6* transgenic plants showed that the binding affinity of LHP1 was enhanced by a warm ambient temperature (Figures 2H–2K). Additional ChIP-qPCR assays in *proLHP1::gLHP1-GFP/ein2-5 lhp1-6* and *proLHP1::gLHP1-GFP/ein3-1 eil1-1 lhp1-6* demonstrated that warm-ambient-temperature-induced LHP1 binding was largely compromised by the mutations of EIN2 and EIN3/EIL1 (Figures 2H–2K). Given that EIN2-C directly associates with LHP1, we conducted EIN2-C ChIP assays with the long-arm cross-linker ethylene glycol bis(succinimidyl succinate) (EGS). The result showed that EIN2-C was enriched in LHP1-bound chromatin regions (Figures S4O–S4R). Interestingly, EIN2 binding could be detected at some of the EIN3-bound regions after warm ambient temperature treatment (Figures S4O–S4R), indicating the co-functions of EIN2 and EIN3 in response to warm ambient temperatures. Notably, the enrichment of EIN2-C on chromatin was significantly reduced in the *lhp1-3* mutant, suggesting that LHP1 is crucial for directing EIN2-C to specific chromatin regions in response to warm ambient temperatures (Figures S4O–S4R). Taken together, these data provide compelling evidence that EIN2, EIN3, and LHP1 collectively function in the same complex on a subset of genes that are responsible for the warm ambient temperature response. Additionally, there is a mutual regulatory interaction between EIN3 and LHP1 in their binding activities.

Chromatin bivalence plays key roles in EIN2-, EIN3-, and LHP1-dependent warm ambient temperature response

LHP1 is considered as a component of both PRC1 and PRC2 and known to recognize H3K27me3 histone tails.^{40–42} We therefore examined H3K27me3 levels over those EIN2-LHP1-dependent DEGs using publicly available H3K27me3 ChIP-seq data.⁴³ Intriguingly, H3K27me3 histone marks were highly enriched over those DEGs (Figure 3A), which is in contrast with the canonical role of H3K27me3 as a transcriptional repression mark.^{44,45} Many studies have shown that the H3K27me3-marked chromatin regions can co-exist with active histone modifications, such as H3K4me3, to establish a bivalent epigenetic state for rapid gene regulation in response to various internal or external signals.^{46–48} Therefore, we examined H3K4me3 over EIN2-LHP1-dependent DEGs using published ChIP-seq data (Figure 3B).⁴⁹ 42 of the EIN2-LHP1-dependent genes are characterized as bivalent genes, and 25 of these bivalent genes have EIN3 binding motifs (Figures 3C and S5A–S5D). More importantly, most of the 25 genes have been reported to play essential functions in plant growth and stress response, indicating that EIN2, EIN3, and LHP1 target a key subset of bivalent genes in

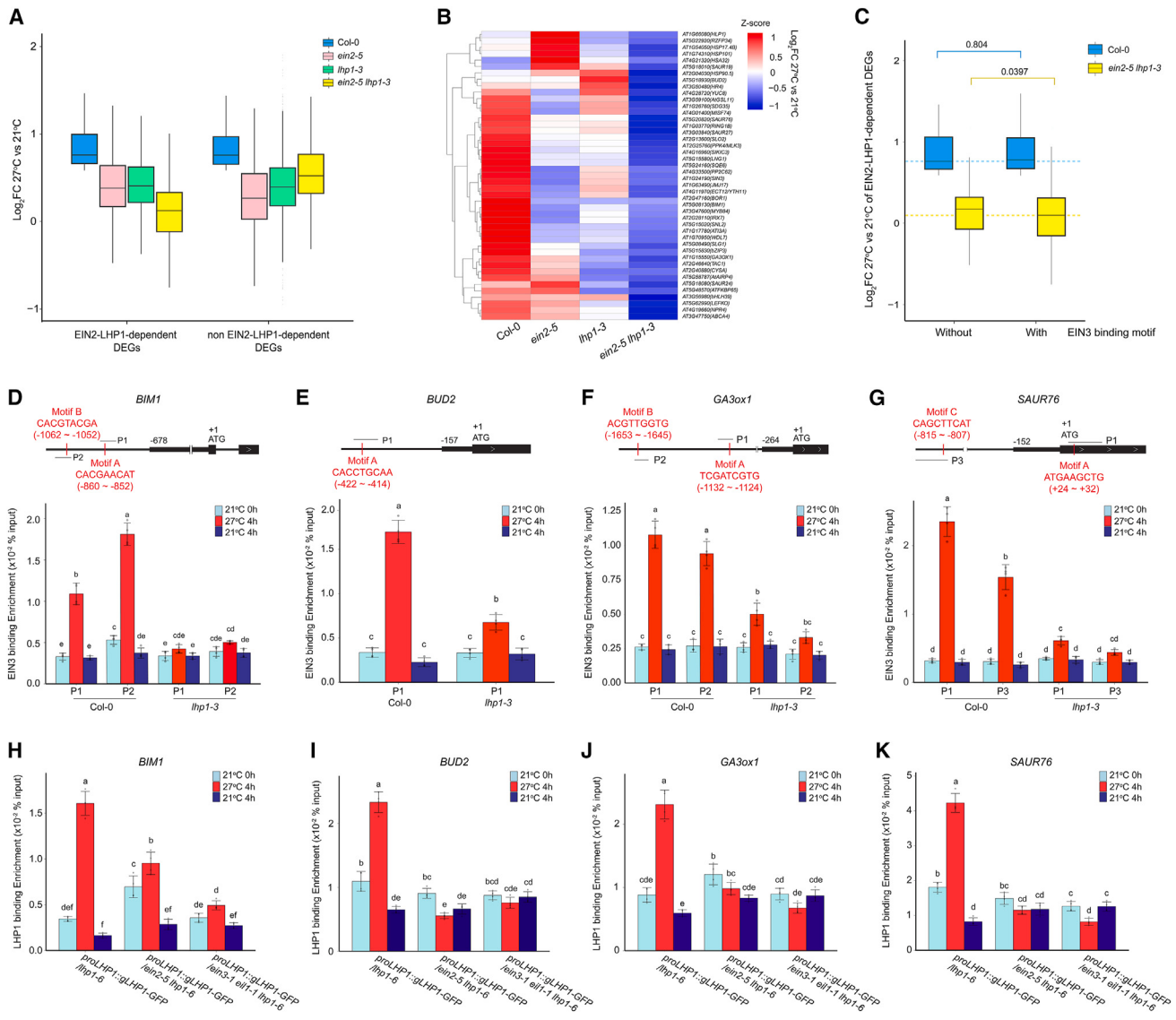


Figure 2. EIN2, EIN3, and LHP1 collectively regulate the warm ambient temperature response at the transcription level

(A) Boxplots to compare the expression of EIN2-LHP1-dependent warm-ambient-temperature-induced DEGs versus those genes that are EIN2-LHP1 independent in Col-0, *ein2-5*, *lhp1-3*, and *ein2-5 lhp1-3* plants.

(B) Heatmap to show the transcriptional responsiveness to warm ambient temperature of key EIN2-LHP1 co-dependent DEGs in Col-0 and the indicated plants. Z score-transformed log₂FC value of each gene was used to plot the heatmap.

(C) Boxplots to compare the reduction of transcriptional activation in the EIN2-LHP1 co-dependent DEGs with EIN3 binding motif versus without EIN3 binding motif in Col-0 and *ein2-5 lhp1-3* plants. *p* values were determined by a two-tailed t test.

(D–G) ChIP-qPCR assay to detect EIN3 enrichment at EIN3 binding motifs in the target genes. Top: diagrams to show the locations of ChIP-qPCR primers in the promoter regions of each target gene. Red vertical lines indicate EIN3 binding motifs. Black bracelets indicate the location of ChIP-qPCR amplicons. Chromatins isolated from 5-day-old seedlings collected at 21°C before treatments, 27°C treatments for 4 h, and 21°C control treatments for 4 h were immunoprecipitated with anti-EIN3.

(H-K) ChIP-qPCR assays to examine the enrichment of LHP1 on the target genes in the indicated genetic backgrounds. Five-day-old seedlings were collected at 21°C before treatments, 27°C treatments for 4 h, and 21°C control treatments for 4 h and subjected to ChIP assay with anti-GFP. The locations of ChIP-qPCR amplicons are indicated in Figures S4K-S4N.

For (D)–(K), data represent the mean \pm SD of at least three replicates, and the original percentages of the input values are plotted as dots. The statistically significant differences of EIN3 or LHP1 binding in different conditions and genetic backgrounds were calculated by a one-way ANOVA test followed by Tukey's HSD test with $p \leq 0.05$.

See also Figures S2E, S2F, S3, S1, and S4.

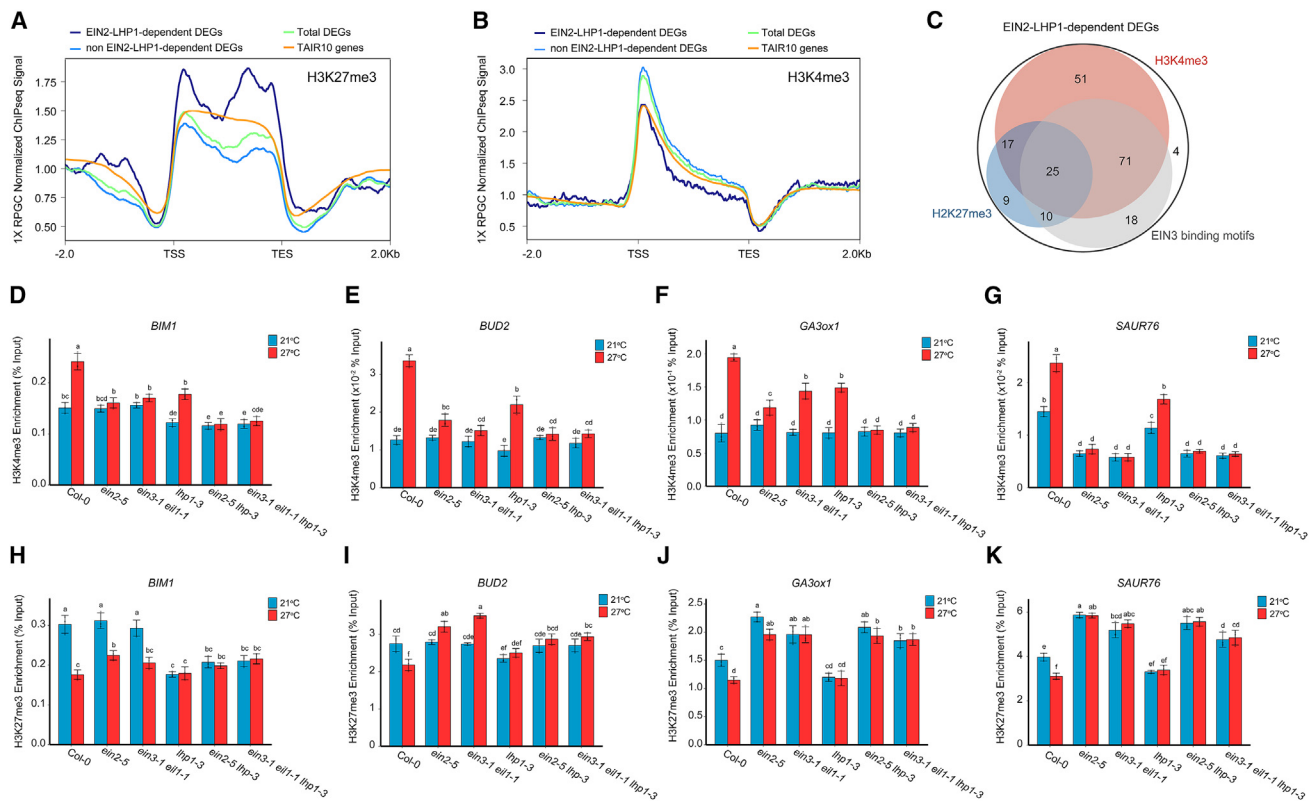


Figure 3. EIN2, EIN3, and LHP1 co-regulate bivalent chromatin for warm-ambient-temperature-induced transcriptional activation

(A and B) Profile plots of the 1x normalization (reads per genomic content, RPGC)-normalized H3K27me3 (A) and H3K4me3 (B) ChIP-seq signals over EIN2-LHP1 co-dependent warm-ambient-temperature-induced DEGs, non-EIN2-LHP1 co-dependent warm-ambient-temperature-induced DEGs, total warm-ambient-temperature-induced DEGs, and total TAIR10-annotated genes. TSS, transcription start site; TES, transcription end site.

(C) Venn diagram to compare the H3K27me3-marked DEGs, H3K4me3-marked DEGs, and DEGs identified with EIN3 binding motifs in EIN2-LHP1 co-dependent warm-ambient-temperature-induced DEGs.

(D–K) ChIP-qPCR analyses to evaluate the enrichment of H3K4me3 (D–G) and H3K27me3 (H–K) in Col-0, *ein2-5*, *ein3-1 eil1-1*, *lhp1-3*, *ein2-5 lhp1-3*, and *ein3-1 eil1-1 lhp1-3* 5-day-old green seedlings treated with 27°C for 4 h or kept in 21°C for 4 h of selected genes. The individual data point of the methylated histone enrichment relative to input is plotted as a dot. Different letters indicate statistically significant differences ($p \leq 0.05$) between each experiment group calculated by a one-way ANOVA test followed by Tukey's HSD test.

See also Figure S5.

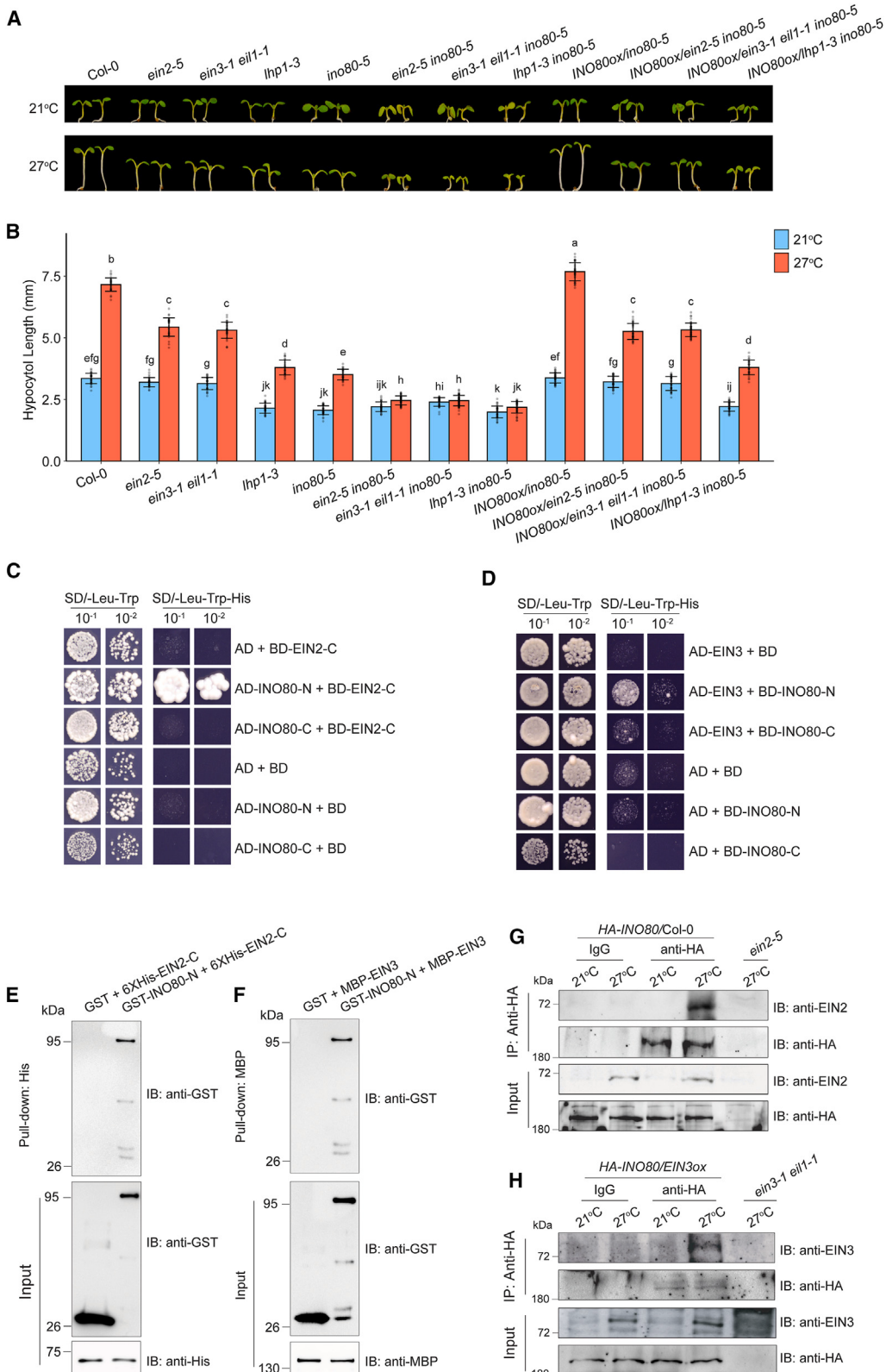
response to high ambient temperatures (Figure S5E).^{13,35–38,50–59} Sequential ChIP-qPCR (Re-ChIP) assays of anti-H3K4me3 ChIP followed by anti-H3K27me3 ChIP using Col-0 seedlings with or without warm ambient temperature treatment further confirmed that H3K4me3 and H3K27me3 indeed co-exist on the same chromatin regions of those target genes (Figures S5F–S5I).

To assess the dynamics of H3K4me3 and H3K27me3 in response to warm ambient temperatures in those bivalence genes, we performed ChIP-qPCR assays in the selected target genes. H3K4me3 levels were elevated by warm ambient temperature treatment in Col-0 (Figures 3D–3G). However, the elevations were significantly reduced in *ein2-5*, *ein3-1 eil1-1*, and *lhp1-3* mutants. Notably, the elevation was nearly undetectable in both *ein2-5 lhp1-3* and *ein3-1 eil1-1 lhp1-3* mutants (Figures 3D–3G). In contrast, H3K27me3 levels showed a slight reduction or remained similar to those in normal temperatures in Col-0 in response to warm ambient temperatures (Figures 3H–3K). The reduction of H3K27me3 levels was abolished in *ein2-5*- and *ein3-1 eil1-1*-related mutants. Additionally,

our Re-ChIP assays revealed a significant decrease of H3K27me3 enrichment immunoprecipitated by anti-H3K4me3 in Col-0 after 27°C treatment, shown as the ratio of the second round of IP by H3K27me3 to the first round of IP by H3K4me3 (IP2 H3K27me3/IP1 H3K4me3), indicating that the warm ambient temperature induced chromatin bivalency switching (Figures S5F–S5I). However, this decrease in the IP2 H3K27me3/IP1 H3K4me3 ratio after 27°C treatment was not found in the *ein2-5 lhp1-3* double mutant (Figures S5F–S5I). Altogether, these results demonstrate that EIN2, EIN3, and LHP1 collectively regulate warm-ambient-temperature-induced H3K4me3 elevation to counteract repressive mark H3K27me3, facilitating gene transcriptional activation in bivalent chromatin.

INO80 associates with EIN2 and EIN3 to regulate warm ambient temperature response

Mutations in INO80 lead to a reduction in the warm ambient temperature response, and INO80 is involved in the regulation of H3K4me3 deposition for active transcription for



(legend on next page)

thermomorphogenesis.²⁴ Therefore, we decided to evaluate the involvement of INO80 in the ethylene-mediated warm ambient temperature response. We generated *ein2-5 ino80-5* double mutants and *ein3-1 eil1-1 ino80-5* triple mutants, and warm ambient temperature response phenotypic assays showed that the partial irresponsiveness of *ein2-5*, *ein3-1 eil1-1*, and *ino80-5* was significantly enhanced in the *ein2-5 ino80-5* and *ein3-1 eil1-1 ino80-5* mutants (Figures 4A and 4B). We also generated an *lhp1-3 ino80-5* double mutant and observed that it showed a similar defective warm ambient temperature response to that observed in the *ein2-5 ino80-5* and *ein3-1 eil1-1 ino80-5* mutants (Figures 4A and 4B). Moreover, the adult plants of *ein2-5 ino80-5*, *ein3-1 eil1-1 ino80-5*, and *lhp1-3 ino80-5* exhibited a severe developmental defect when compared to *lhp1-3* and *ino80-5* single mutants and Col-0 (Figure S6A). Additionally, the reduced warm ambient temperature response in *ein2-5 ino80-5*, *ein3-1 eil1-1 ino80-5*, and *lhp1-3 ino80-5* mutants was rescued by over-expressing *INO80*, further confirming that the mutation in *INO80* leads to additive defects for the warm ambient temperature response in *ein2-5*, *ein3-1 eil1-1*, and *lhp1-3* mutants, respectively (Figures 4A, 4B, and S6B). Overall, these results demonstrate the genetic interactions among EIN2, EIN3, LHP1, and INO80 in response to warm ambient temperatures.

We then explored the potential physical interaction between INO80 and EIN2 or EIN3. We performed Y2H assays and found that the N terminus of INO80 (INO80-N) can interact with both EIN2-C and EIN3 *in vitro* (Figures 4C, 4D, and S6C–S6E). We then conducted *in vitro* pull-down assays using purified proteins from *E. coli*. The result confirmed the interaction between EIN2-C and INO80-N and the interaction between EIN3 and INO80-N (Figures 4E and 4F). Further *in vivo* colP assays showed that INO80 interacted with EIN2-C or EIN3 when seedlings were subjected to 4 h of warm ambient temperature treatment (Figures 4G, 4H, and S6F). To further evaluate the functional interaction of INO80 with EIN2, EIN3, and LHP1, we first examined the target gene expression in *INO80*-related mutants in response to a warm ambient temperature. The result showed that the warm-ambient-temperature-induced activation of target genes was reduced in the *ino80-5* mutant, and this reduction was further enhanced in *ein2-5 ino80-5*, *ein3-1 eil1-1 ino80-5*, and *lhp1-3 ino80-5* mutants (Figures S7A–S7D). We then examined H3K4me3 and H3K27me3 levels in the target genes in Col-0 and *ino80-5*. ChIP-qPCR results showed that H3K4me3 levels

were decreased in *ino80-5* both with and without warm ambient temperature treatments compared to those in Col-0 (Figure 5A). In contrast, no significant differences in H3K27me3 levels were detected between *ino80-5* and Col-0 under normal conditions. However, the warm-ambient-temperature-induced reduction detected in Col-0 was diminished in *ino80-5* (Figure 5B).

Since INO80 interacts with EIN3 and is associated with H3K4me3, we tested the INO80 binding at both EIN3 binding motifs and transcription start site (TSS) regions of target genes in the ChIP-qPCR assays. Remarkably, INO80 displayed an increased binding affinity to the target genes under warm ambient temperatures, while INO80 protein levels remained unchanged (Figures 5C–5F and S6D). Moreover, INO80 binding was significantly reduced when *EIN2*, *EIN3*, or *LHP1* was mutated (Figures 5C–5F). Accordingly, overexpression of INO80 is not sufficient to increase H3K4me3 levels in the absence of EIN2, EIN3, and LHP1 in response to a warm ambient temperature (Figures S7E–S7H). Furthermore, ChIP-qPCR assays showed that INO80 had no effect on the H3K27me3 levels in *BUD2*, *GA3ox1*, and *SAUR76* (Figures S7J–S7L), supporting our hypothesis that EIN2 and EIN3 recruit INO80 to LHP1-EIN2 and EIN3 co-targeted chromatin regions to regulate H3K4me3, but not H3K27me3, levels. However, we noticed a smaller effect of INO80 in regulating H3K27me3 levels in *BIM1* (Figure S7I). Finally, we explored whether INO80 regulates EIN3 binding, given the fact that activated bivalent chromatin regions have been shown to gain accessibility for TF binding to activate gene expression.^{60–62} In the absence of INO80, the binding of EIN3 to selected target genes was decreased, although there is no difference in its protein level in Col-0 and in *ino80-5* (Figure S7M–S7Q). Altogether, our results demonstrate that EIN2 and EIN3 collaborate with INO80 at specific bivalent targets to enhance H3K4me3 enrichment, facilitating the activation of gene expression in response to warm ambient temperatures.

DISCUSSION

With increasing global temperatures, warm ambient temperatures have become an unprecedented abiotic stress that affects plant growth and development. Understanding how plants respond to warm ambient temperatures is crucial for cultivating climate-resilient crops that are more tolerant to high temperature conditions. As a growth and stress hormone, ethylene is vital for

Figure 4. INO80 functions with EIN2 and EIN3 by protein-protein interactions for the warm ambient temperature response

(A) Photographs of representative 5-day-old green seedlings of Col-0, *ein2-5*, *ein3-1 eil1-1*, *lhp1-3*, *ino80-5*, *ein2-5 ino80-5*, *ein3-1 eil1-1 ino80-5*, *lhp1-3 ino80-5*, and complementation lines by 35S::*INO80* grown on MS medium at 21°C and 27°C.

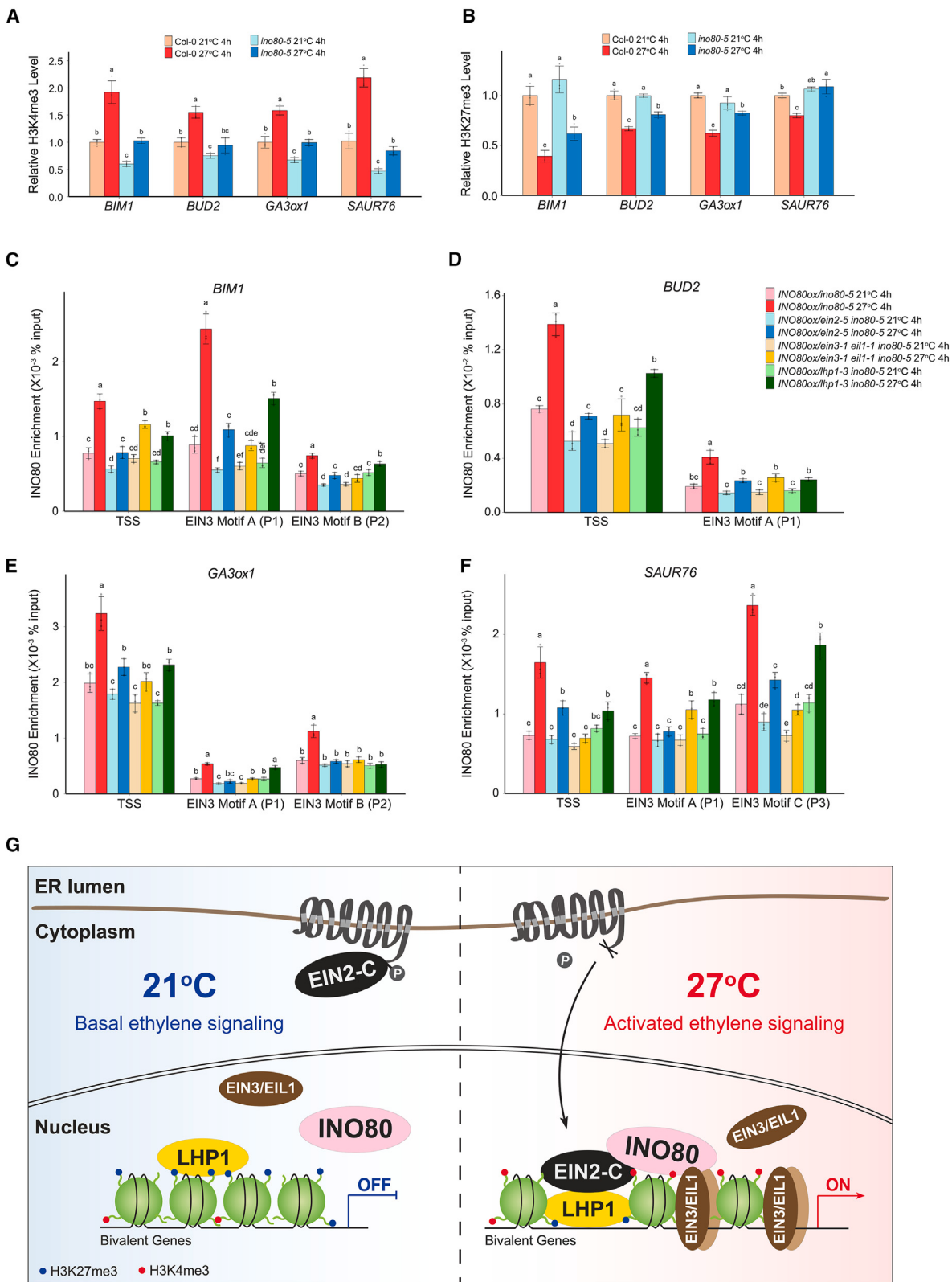
(B) Measurements of hypocotyl lengths from indicated plants in (A). Each value is means ± SD of at least 30 seedlings. Different letters indicate the statistically significant differences between different genotypes and treatments with $p \leq 0.05$ calculated by a one-way ANOVA test and followed by Tukey's HSD test for multiple comparisons.

(C and D) Y2H assay to examine the interaction of INO80 (truncated INO80-N and INO80-C) with EIN2 (C) and EIN3 (D). AD, GAL4 activation domain; BD, GAL4 DNA binding domain. Left: yeasts grown on two-dropout medium as a loading control. Right: yeasts grown on selective three-dropout medium.

(E and F) *In vitro* pull-down assays to examine the interaction between EIN2-C and INO80-N (E) and the interaction between EIN3 and INO80-N (F). *In vitro* purified proteins from *E. coli* were applied for the assays.

(G and H) *In vivo* colP assays of INO80 with EIN2 (G) and INO80 with EIN3 (H). The total protein extracts from 5-day-old seedlings of 35S::HA-INO80/Col-0 (G) or crossed 35S::HA-INO80/EIN3ox (H) transgenic plants treated with 4 h at 21°C or 27°C were immunoprecipitated with anti-HA. The immunoprecipitated proteins were detected by immunoblotting using anti-HA, anti-EIN2, and anti-EIN3, respectively. The input serves as the loading control. IB, immunoblotting; IP, immunoprecipitation.

See also Figure S6.



(legend on next page)

plant adaptations to environmental changes.^{15,63,64} However, the molecular mechanisms by which ethylene regulates the warm ambient temperature response are still largely unknown. In this study, we reveal that LHP1 and INO80 cooperate with ethylene signaling for warm ambient temperature response by activating specific bivalent genes. Firstly, both our genetic and molecular results clearly showed that ethylene signaling and LHP1 share a similar regulation pattern in response to warm ambient temperature (Figures 1 and S1). More importantly, our genetic results showed the synergistic regulation of LHP1 with EIN2 and EIN3 in the warm ambient temperature response (Figures 1 and 2). As LHP1 is a component of PRCs that is potentially involved in the regulation of H3K27me3 and functions as a H3K27me3 reader,^{40,42} our discovery established a link between ethylene signaling and H3K27me3 in the warm ambient temperature response. Interestingly, the genes that are activated by both LHP1 and ethylene signaling in response to warm ambient temperatures have a relatively higher level of H3K27me3 enrichment (Figure 3A), which is contrary to the classical function of H3K27m3 as a transcriptional repression mark.⁶⁵ Our epigenetic profiling analyses showed that the subset of warm-ambient-temperature-responsive DEGs whose transcriptional activation requires EIN2, EIN3, and LHP1 are marked with both H3K4me3 and H3K27me3 (Figures 3A–3C). More importantly, H3K4me3 is elevated by warm ambient temperatures to counteract H3K27me3 for transcriptional activation, which requires all EIN2, EIN3, and LHP1 (Figure 3). Furthermore, we identified INO80 as an important factor that co-binds with the LHP1-EIN2-EIN3 module to promote H3K4me3 deposition for transcription activation (Figures 4 and 5). Overall, our findings highlight the importance of the ethylene signaling pathway and its coordination with bivalent chromatin regulation for gene transcription in response to warm ambient temperatures (Figure 5G).

Chromatin regulation plays a major role in plants' perception, response, and adaptation to temperature changes.²² For example, the exclusion of the histone variant H2A.Z from nucleosomes enhances chromatin accessibility, leading to differential gene expression under elevated temperatures.^{12,24,66} Moreover, histone methylation H3K4me3 has been reported to promote thermal-induced transcription activation.²⁴ However, it is not clear whether and how bivalent histone marks function in the warm ambient temperature response. Bivalent marks are often associated with genes that are important for cell fate decisions, particularly during development processes and cell differentia-

tion.^{46,67,68} A recent study showed that the H3K27me3-H3K18ac bivalent chromatin plays an important role in controlling the timely induction of camalexin biosynthesis gene expression upon pathogen infection in plants.⁶⁹ Cold treatment has also been found to promote the global deposition of the bivalent H3K4me3-H3K27me3 marks over actively transcribed genes in both *Arabidopsis* and potato.^{70,71} A set of dehydration stress memory genes are also labeled with both H3K27me3 and H3K4me3, enabling a rapid and dynamic environmental response.⁷² These recent studies set up examples of bivalent chromatin regulation in plant stress response. In our study, we revealed the coordination between ethylene signaling and chromatin regulators LHP1 and INO80 in orchestrating chromatin bivalency for the warm ambient temperature response. Very interestingly, LHP1 is considered a factor for transcription repression. Yet in our study, the result showed that it is involved in transcriptional activation. A few years ago, Rizzardi et al. showed that LHP1 regulates auxin biosynthesis through the positive regulation of *YUC* genes.⁷³ Veluchamy et al. showed that LHP1 could also be an activator of transcription through differential expression analysis of LHP1-target genes in *lhp1* mutants versus wild-types.⁷⁴ The possible reason is that the presence of bivalent marks at LHP1-EIN2-INO80-EIN3-module-targeted genes introduces a layer of complexity to the transcriptional regulation of the warm ambient temperature response, as many key growth-responsive genes and genes responsive to light or hormones exhibit bivalent marks, rendering them highly susceptible to rapid transcriptional activation upon warm ambient temperature exposure (Figure S5E). Therefore, bivalent marks provide an advantage that allows genes to swiftly switch from a basal or repressed transcriptional state to an activated state, facilitating the timely and precise regulation of gene expression in the right timing and context.

During thermomorphogenesis, PIF4 plays a key role in integrating temperature and light signals to the control of hypocotyl growth.^{10,14,75} Moreover, PIF4 relays different plant internal hormonal signals to the transcriptional regulation of multiple high-temperature- and light-responsive genes.^{76,77} When the ambient temperature elevates, the accumulated PIF4 protein promotes auxin biosynthesis and signaling, which leads to hypocotyl elongation and plant growth.^{3,11,13} However, when compared to Col-0, the regulation of the PIF4 protein level by a warm ambient temperature is not altered in *ein2-5*, *ein3-1 eil1-1*, *ein2-5 lhp1-3*, and *ein3-1 eil1-1 lhp1-3* mutants (Figures S2A and S2B),

Figure 5. EIN2 and EIN3 recruit INO80 to bivalent chromatin to elevate H3K4me3 enrichment in response to warm ambient temperatures
(A and B) ChIP-qPCR analyses of H3K4me3 (A) and H3K27me3 (B) enrichments on the target genes in Col-0 and *ino80-5* mutant in response to warm ambient temperature. Col-0 and *ino80-5* seedlings treated for 4 h under 27°C or kept in 21°C for 4 h were used for the ChIP assay.
(C–F) ChIP-qPCR assays to examine the INO80 binding in *INO80ox/ino80-5*, *INO80ox/ein2-5 ino80-5*, *INO80ox/ein3-1 eil1-1 ino80-5*, and *INO80ox/lhp1-3 ino80-5* in response to warm ambient temperature. Primers targeting TSS regions are the same primers used for H3K4me3 and H3K27me3 ChIP-qPCR for each gene. Primers targeting EIN3 binding motifs are the same primers used for EIN3 ChIP-qPCR for each gene in Figures 2H–2K. All data represent means \pm SD of three replicates, and the individual data point was plotted as a dot. Different letters represent significant differences with $p < 0.05$ in the one-way ANOVA test followed by Tukey's HSD test.

(G) A schematic model to illustrate how LHP1 and INO80 cooperate with EIN2 and EIN3 to regulate bivalent chromatin for rapid transcriptional activation in response to warm ambient temperature. In normal temperature conditions, LHP1 binds to H3K27me3 heavily labeled bivalent genes, and those genes are transcribed at the basal level. On the other hand, the warm ambient temperature condition triggers the activation of ethylene signaling, resulting in EIN2 C-terminal cleavage and EIN3 protein accumulation. LHP1 directs EIN2-C to bivalent chromatin, where EIN2-C co-functions with INO80 and EIN3 at a subset of genes with bivalent marks to elevate H3K4me3 enrichment, counteracting the repressive effects of H3K27me3 and ultimately activating gene expression.
See also Figure S7.

suggesting that ethylene regulates the warm ambient temperature response either independently of PIF4 or downstream of PIF4. Our result showed that both EIN2 and EIN3 proteins are accumulated by warm ambient temperatures (Figure S1). Previous study has demonstrated the accumulation of EIN3 in warm ambient temperatures due to the degradation of EBF1 and EBF2 by the RING E3 ligase SDIR1.¹⁹ As ethylene biosynthesis is positively regulated by EIN3,^{78,79} it is possible that accumulated EIN3 leads to an elevation of ethylene biosynthesis, resulting in the accumulation of EIN2 and EIN3 through a positive feedback regulation in response to warm ambient temperatures. It will be interesting to further explore whether PIF4 integrates temperature signals to regulate EIN3 protein stability in response to warm ambient temperatures.

Limitations of the study

Our study revealed that ethylene signaling is involved in the chromatin bivalency switching in response to warm ambient temperatures, yet the detailed molecular mechanisms of how histone methylation is altered are unknown. Isolating histone methyltransferase or the histone demethylase that is involved in this process will be of immediate interest. Additionally, how ethylene signaling is initiated upon the ambient temperature change remains unknown. Identifying the hub where ethylene signaling interacts with cues of warm ambient temperatures will be the next step to understand the involvement of ethylene signaling in the warm ambient temperature response.

RESOURCE AVAILABILITY

Lead contact

Further information and requests for reagents may be directed to and will be fulfilled by the lead contact, Hong Qiao (hqiao@austin.utexas.edu).

Materials availability

Further information and requests for all unique materials generated in this study can be directed to and will be fulfilled by the corresponding author, Hong Qiao (hqiao@austin.utexas.edu).

Data and code availability

The high-throughput sequencing data generated in this study have been deposited in the GEO database (GEO: GSE256453). This paper does not report original code. Any additional information required to reanalyze the data in this study is available from the [lead contact](#) upon request.

ACKNOWLEDGMENTS

We thank C. Dean for sharing the *proLHP1::gLHP1-GFP/lhp1-6 FRI* seeds. We thank D. Jiang for sharing the 35S::HA-*INO80/ino80-5* and *ino80-5* seeds. We thank J. Kim and S. Sung for suggestions on the experimental design. This work was supported by grants from the National Institutes of Health to H.Q. (NIH-2R01 GM115879) and the National Science Foundation (MCB-2014408) to E.H.

AUTHOR CONTRIBUTIONS

Z.S. and H.Q. conceived the project and designed the experiments. Z.S. performed most of the experiments and data analyses. Y.B. performed PIF4 immunoblots. Z.S. and H.Q. wrote the manuscript. E.H. advised on the experimental design and the manuscript. All authors read and approved the final manuscript.

DECLARATION OF INTERESTS

The authors declare no competing interests.

STAR★METHODS

Detailed methods are provided in the online version of this paper and include the following:

- KEY RESOURCES TABLE
- EXPERIMENTAL MODEL AND STUDY PARTICIPANT DETAILS
- METHOD DETAILS
 - Plant protein extraction and western blot assays
 - Plant RNA extraction and gene expression analysis
 - mRNA sequencing and data processing
 - Yeast two-hybrid assay
 - Transient expression in *Nicotiana benthamiana* leaves
 - Co-immunoprecipitation
 - ChIP sequencing data analysis
 - ChIP-qPCR assays
- QUANTIFICATION AND STATISTICAL ANALYSIS

SUPPLEMENTAL INFORMATION

Supplemental information can be found online at <https://doi.org/10.1016/j.celrep.2024.114758>.

Received: April 26, 2024

Revised: August 9, 2024

Accepted: August 29, 2024

Published: September 11, 2024

REFERENCES

1. Lippmann, R., Babben, S., Menger, A., Delker, C., and Quint, M. (2019). Development of Wild and Cultivated Plants under Global Warming Conditions. *Curr. Biol.* 29, R1326–R1338. <https://doi.org/10.1016/j.cub.2019.10.016>.
2. Schauberger, B., Archontoulis, S., Arneth, A., Balkovic, J., Ciaias, P., Derzing, D., Elliott, J., Folberth, C., Khabarov, N., Müller, C., et al. (2017). Consistent negative response of US crops to high temperatures in observations and crop models. *Nat. Commun.* 8, 13931. <https://doi.org/10.1038/ncomms13931>.
3. Casal, J.J., and Balasubramanian, S. (2019). Thermomorphogenesis. *Annu. Rev. Plant Biol.* 70, 321–346. <https://doi.org/10.1146/annurev-arplant-050718-095919>.
4. Quint, M., Delker, C., Franklin, K.A., Wigge, P.A., Halliday, K.J., and van Zanten, M. (2016). Molecular and genetic control of plant thermomorphogenesis. *Nat. Plants* 2, 15190. <https://doi.org/10.1038/nplants.2015.190>.
5. Quint, M., Delker, C., Balasubramanian, S., Balcerowicz, M., Casal, J.J., Castroverde, C.D.M., Chen, M., Chen, X., De Smet, I., Fankhauser, C., et al. (2023). 25 Years of thermomorphogenesis research: milestones and perspectives. *Trends Plant Sci.* 28, 1098–1100. <https://doi.org/10.1016/j.tplants.2023.07.001>.
6. Jung, J.-H., Barbosa, A.D., Hutin, S., Kumita, J.R., Gao, M., Derwort, D., Silva, C.S., Lai, X., Pierre, E., Geng, F., et al. (2020). A prion-like domain in ELF3 functions as a thermosensor in Arabidopsis. *Nature* 585, 256–260. <https://doi.org/10.1038/s41586-020-2644-7>.
7. Legris, M., Klose, C., Burgie, E.S., Rojas, C.C.R., Neme, M., Hiltbrunner, A., Wigge, P.A., Schäfer, E., Vierstra, R.D., and Casal, J.J. (2016). Phytochrome B integrates light and temperature signals in Arabidopsis</i>. *Science* 354, 897–900. <https://doi.org/10.1126/science.aaf5656>.
8. Box, M.S., Huang, B.E., Domijan, M., Jaeger, K.E., Khattak, A.K., Yoo, S.J., Sedivy, E.L., Jones, D.M., Hearn, T.J., Webb, A.A.R., et al. (2015).

- ELF3 controls thermoresponsive growth in Arabidopsis. *Curr. Biol.* 25, 194–199. <https://doi.org/10.1016/j.cub.2014.10.076>.
9. Jung, J.-H., Domijan, M., Klose, C., Biswas, S., Ezer, D., Gao, M., Khatkak, A.K., Box, M.S., Charoensawan, V., Cortijo, S., et al. (2016). Phytochromes function as thermosensors in <i>Arabidopsis</i>. *Science* 354, 886–889. <https://doi.org/10.1126/science.aaf6005>.
 10. Lee, S., Wang, W., and Huq, E. (2021). Spatial regulation of thermomorphogenesis by HY5 and PIF4 in Arabidopsis. *Nat. Commun.* 12, 3656. <https://doi.org/10.1038/s41467-021-24018-7>.
 11. Franklin, K.A., Lee, S.H., Patel, D., Kumar, S.V., Spartz, A.K., Gu, C., Ye, S., Yu, P., Breen, G., Cohen, J.D., et al. (2011). PHYTOCHROME-INTERACTING FACTOR 4 (PIF4) regulates auxin biosynthesis at high temperature. *Proc. Natl. Acad. Sci. USA* 108, 20231–20235. <https://doi.org/10.1073/pnas.1110682108>.
 12. Kumar, S.V., Lucyshyn, D., Jaeger, K.E., Alós, E., Alvey, E., Harberd, N.P., and Wigge, P.A. (2012). Transcription factor PIF4 controls the thermosensory activation of flowering. *Nature* 484, 242–245. <https://doi.org/10.1038/nature10928>.
 13. Sun, J., Qi, L., Li, Y., Chu, J., and Li, C. (2012). PIF4-Mediated Activation of YUCCA8 Expression Integrates Temperature into the Auxin Pathway in Regulating Arabidopsis Hypocotyl Growth. *PLoS Genet.* 8, e1002594. <https://doi.org/10.1371/journal.pgen.1002594>.
 14. Proveniers, M.C.G., and van Zanten, M. (2013). High temperature acclimation through PIF4 signaling. *Trends Plant Sci.* 18, 59–64. <https://doi.org/10.1016/j.tplants.2012.09.002>.
 15. Huang, J., Zhao, X., Bürger, M., Chory, J., and Wang, X. (2023). The role of ethylene in plant temperature stress response. *Trends Plant Sci.* 28, 808–824. <https://doi.org/10.1016/j.tplants.2023.03.001>.
 16. Larkindale, J., Hall, J.D., Knight, M.R., and Vierling, E. (2005). Heat stress phenotypes of Arabidopsis mutants implicate multiple signaling pathways in the acquisition of thermotolerance. *Plant Physiol.* 138, 882–897. <https://doi.org/10.1104/pp.105.062257>.
 17. Larkindale, J., and Huang, B. (2005). Effects of Abscisic Acid, Salicylic Acid, Ethylene and Hydrogen Peroxide in Thermotolerance and Recovery for Creeping Bentgrass. *Plant Growth Regul.* 47, 17–28. <https://doi.org/10.1007/s10725-005-1536-z>.
 18. John, S., Apelt, F., Kumar, A., Acosta, I.F., Bents, D., Annunziata, M.G., Fichtner, F., Gutjahr, C., Mueller-Roeber, B., and Olas, J.J. (2023). The transcription factor HSFA7b controls thermomemory at the shoot apical meristem by regulating ethylene biosynthesis and signaling in Arabidopsis. *Plant Communications* 5, 100743. <https://doi.org/10.1016/j.xplc.2023.100743>.
 19. Hao, D., Jin, L., Wen, X., Yu, F., Xie, Q., and Guo, H. (2021). The RING E3 ligase SDIR1 destabilizes EBF1/EBF2 and modulates the ethylene response to ambient temperature fluctuations in Arabidopsis. *Proc. Natl. Acad. Sci. USA* 118, e2024592118. <https://doi.org/10.1073/pnas.2024592118>.
 20. Cheng, Y.-J., Wang, J.-W., and Ye, R. (2024). Histone dynamics responding to internal and external cues underlying plant development. *Plant Physiol.* 194, 1980–1997. <https://doi.org/10.1093/plphys/kiad676>.
 21. He, K., Cao, X., and Deng, X. (2021). Histone methylation in epigenetic regulation and temperature responses. *Curr. Opin. Plant Biol.* 61, 102001. <https://doi.org/10.1016/j.pbi.2021.102001>.
 22. Perrella, G., Bäurle, I., and van Zanten, M. (2022). Epigenetic regulation of thermomorphogenesis and heat stress tolerance. *New Phytol.* 234, 1144–1160. <https://doi.org/10.1111/nph.17970>.
 23. Kumar, S.V., and Wigge, P.A. (2010). H2A.Z-containing nucleosomes mediate the thermosensory response in Arabidopsis. *Cell* 140, 136–147. <https://doi.org/10.1016/j.cell.2009.11.006>.
 24. Xue, M., Zhang, H., Zhao, F., Zhao, T., Li, H., and Jiang, D. (2021). The INO80 chromatin remodeling complex promotes thermomorphogenesis by connecting H2A.Z eviction and active transcription in Arabidopsis. *Mol. Plant* 14, 1799–1813. <https://doi.org/10.1016/j.molp.2021.07.001>.
 25. van der Woude, L.C., Perrella, G., Snoek, B.L., van Hoogdalem, M., Novák, O., van Verk, M.C., van Kooten, H.N., Zorn, L.E., Tonckens, R., Dongus, J.A., et al. (2019). HISTONE DEACETYLASE 9 stimulates auxin-dependent thermomorphogenesis in *Arabidopsis thaliana* by mediating H2A.Z depletion. *Proc. Natl. Acad. Sci. USA* 116, 25343–25354. <https://doi.org/10.1073/pnas.1911694116>.
 26. Tasset, C., Singh Yadav, A., Sureshkumar, S., Singh, R., van der Woude, L., Nekrasov, M., Tremethick, D., van Zanten, M., and Balasubramanian, S. (2018). POWERDRESS-mediated histone deacetylation is essential for thermomorphogenesis in *Arabidopsis thaliana*. *PLoS Genet.* 14, e1007280. <https://doi.org/10.1371/journal.pgen.1007280>.
 27. Kim, J., Bordiyya, Y., Kathare, P.K., Zhao, B., Zong, W., Huq, E., and Sung, S. (2021). Phytochrome B triggers light-dependent chromatin remodeling through the PRC2-associated PHD finger protein VIL1. *Nat. Plants* 7, 1213–1219. <https://doi.org/10.1038/s41477-021-00986-y>.
 28. Kim, J., Bordiyya, Y., Xi, Y., Zhao, B., Kim, D.H., Pyo, Y., Zong, W., Ricci, W.A., and Sung, S. (2023). Warm temperature-triggered developmental reprogramming requires VIL1-mediated, genome-wide H3K27me3 accumulation in Arabidopsis. *Development* 150, dev201343. <https://doi.org/10.1242/dev.201343>.
 29. Cui, X., Zheng, Y., Lu, Y., Issakidis-Bourguet, E., and Zhou, D.X. (2021). Metabolic control of histone demethylase activity involved in plant response to high temperature. *Plant Physiol.* 185, 1813–1828. <https://doi.org/10.1093/plphys/kiab020>.
 30. He, K., Mei, H., Zhu, J., Qiu, Q., Cao, X., and Deng, X. (2022). The histone H3K27 demethylase REF6/JMJ12 promotes thermomorphogenesis in Arabidopsis. *Natl. Sci. Rev.* 9, nwab213. <https://doi.org/10.1093/nsr/nwab213>.
 31. Fonouni-Farde, C., Christ, A., Blein, T., Legascue, M.F., Ferrero, L., Moison, M., Lucero, L., Ramírez-Prado, J.S., Latrasse, D., Gonzalez, D., et al. (2022). The Arabidopsis APOLO and human UPAT sequence-unrelated long noncoding RNAs can modulate DNA and histone methylation machineries in plants. *Genome Biol.* 23, 181. <https://doi.org/10.1186/s13059-022-02750-7>.
 32. Stepanova, A.N., Yun, J., Likhacheva, A.V., and Alonso, J.M. (2007). Multilevel Interactions between Ethylene and Auxin in Arabidopsis Roots. *Plant Cell* 19, 2169–2185. <https://doi.org/10.1105/tpc.107.052068>.
 33. Yang, H., Berry, S., Olsson, T.S.G., Hartley, M., Howard, M., and Dean, C. (2017). Distinct phases of Polycomb silencing to hold epigenetic memory of cold in Arabidopsis. *Science* 357, 1142–1145. <https://doi.org/10.1126/science.aan1121>.
 34. Chang, K.N., Zhong, S., Weirauch, M.T., Hon, G., Pelizzola, M., Li, H., Huang, S.-s.C., Schmitz, R.J., Urich, M.A., Kuo, D., et al. (2013). Temporal transcriptional response to ethylene gas drives growth hormone cross-regulation in Arabidopsis. *Elife* 2, e00675. <https://doi.org/10.7554/elife.00675>.
 35. Liang, T., Mei, S., Shi, C., Yang, Y., Peng, Y., Ma, L., Wang, F., Li, X., Huang, X., Yin, Y., and Liu, H. (2018). UVR8 Interacts with BES1 and BIM1 to Regulate Transcription and Photomorphogenesis in Arabidopsis. *Dev. Cell* 44, 512–523.e5. <https://doi.org/10.1016/j.devcel.2017.12.028>.
 36. Cui, X., Ge, C., Wang, R., Wang, H., Chen, W., Fu, Z., Jiang, X., Li, J., and Wang, Y. (2010). The BUD2 mutation affects plant architecture through altering cytokinin and auxin responses in Arabidopsis. *Cell Res.* 20, 576–586. <https://doi.org/10.1038/cr.2010.51>.
 37. Stavang, J.A., Gallego-Bartolomé, J., Gómez, M.D., Yoshida, S., Asami, T., Olsen, J.E., García-Martínez, J.I., Alabadí, D., and Blázquez, M.A. (2009). Hormonal regulation of temperature-induced growth in Arabidopsis. *Plant J.* 60, 589–601. <https://doi.org/10.1111/j.1365-313X.2009.03983.x>.
 38. Markakis, M.N., Boron, A.K., Van Loock, B., Saini, K., Cirera, S., Verbeelen, J.-P., and Vissenberg, K. (2013). Characterization of a Small Auxin-Up RNA (SAUR)-Like Gene Involved in Arabidopsis thaliana

- Development. *PLoS One* 8, e82596. <https://doi.org/10.1371/journal.pone.0082596>.
39. Molitor, A.M., Latrasse, D., Zytnicki, M., Andrey, P., Houba-Hérin, N., Hauchet, M., Battail, C., Del Prete, S., Alberti, A., Quesneville, H., and Gaudin, V. (2016). The Arabidopsis hnRNP-Q Protein LIF2 and the PRC1 Subunit LHP1 Function in Concert to Regulate the Transcription of Stress-Responsive Genes. *Plant Cell* 28, 2197–2211. <https://doi.org/10.1105/tpc.16.00244>.
 40. Liu, Y., Yang, X., Zhou, M., Yang, Y., Li, F., Yan, X., Zhang, M., Wei, Z., Qin, S., and Min, J. (2022). Structural basis for the recognition of methylated histone H3 by the Arabidopsis LHP1 chromodomain. *J. Biol. Chem.* 298, 101623. <https://doi.org/10.1016/j.jbc.2022.101623>.
 41. Zhang, X., Germann, S., Blus, B.J., Khorasanizadeh, S., Gaudin, V., and Jacobsen, S.E. (2007). The Arabidopsis LHP1 protein colocalizes with histone H3 Lys27 trimethylation. *Nat. Struct. Mol. Biol.* 14, 869–871. <https://doi.org/10.1038/nsmb1283>.
 42. Turck, F., Roudier, F., Farrona, S., Martin-Magniette, M.-L., Guillaume, E., Buisine, N., Gagnot, S., Martienssen, R.A., Coupland, G., and Colot, V. (2007). Arabidopsis TFL2/LHP1 Specifically Associates with Genes Marked by Trimethylation of Histone H3 Lysine 27. *PLoS Genet.* 3, e86. <https://doi.org/10.1371/journal.pgen.0030086>.
 43. Yin, X., Romero-Campero, F.J., de Los Reyes, P., Yan, P., Yang, J., Tian, G., Yang, X., Mo, X., Zhao, S., Calonje, M., and Zhou, Y. (2021). H2AK121ub in Arabidopsis associates with a less accessible chromatin state at transcriptional regulation hotspots. *Nat. Commun.* 12, 315. <https://doi.org/10.1038/s41467-020-20614-1>.
 44. Wiles, E.T., and Selker, E.U. (2017). H3K27 methylation: a promiscuous repressive chromatin mark. *Curr. Opin. Genet. Dev.* 43, 31–37. <https://doi.org/10.1016/j.gde.2016.11.001>.
 45. Young, M.D., Willson, T.A., Wakefield, M.J., Trounson, E., Hilton, D.J., Blewitt, M.E., Oshlack, A., and Majewski, I.J. (2011). ChIP-seq analysis reveals distinct H3K27me3 profiles that correlate with transcriptional activity. *Nucleic Acids Res.* 39, 7415–7427. <https://doi.org/10.1093/nar/gkr416>.
 46. Bernstein, B.E., Mikkelsen, T.S., Xie, X., Kamal, M., Huebert, D.J., Cuff, J., Fry, B., Meissner, A., Wernig, M., Plath, K., et al. (2006). A bivalent chromatin structure marks key developmental genes in embryonic stem cells. *Cell* 125, 315–326. <https://doi.org/10.1016/j.cell.2006.02.041>.
 47. Voigt, P., Tee, W.W., and Reinberg, D. (2013). A double take on bivalent promoters. *Genes Dev.* 27, 1318–1338. <https://doi.org/10.1101/gad.219626.113>.
 48. Gao, Z., Li, Y., Ou, Y., Yin, M., Chen, T., Zeng, X., Li, R., and He, Y. (2023). A pair of readers of bivalent chromatin mediate formation of Polycomb-based "memory of cold" in plants. *Mol. Cell* 83, 1109–1124.e4. <https://doi.org/10.1016/j.molcel.2023.02.014>.
 49. Chica, C., Szarzynska, B., Chen-Min-Tao, R., Duvernois-Berthet, E., Kassam, M., Colot, V., and Roudier, F. (2013). Profiling spatial enrichment of chromatin marks suggests an additional epigenomic dimension in gene regulation. *Front. Life Sci.* 7, 80–87. <https://doi.org/10.1080/21553769.2013.844734>.
 50. Izhaki, A., and Bowman, J.L. (2007). KANADI and Class III HD-Zip Gene Families Regulate Embryo Patterning and Modulate Auxin Flow during Embryogenesis in Arabidopsis. *Plant Cell* 19, 495–508. <https://doi.org/10.1105/tpc.106.047472>.
 51. Wang, Z., Kang, J., Armando Casas-Mollano, J., Dou, Y., Jia, S., Yang, Q., Zhang, C., and Cerutti, H. (2021). MLK4-mediated phosphorylation of histone H3T3 promotes flowering by transcriptional silencing of FLC/MAF in Arabidopsis thaliana. *Plant J.* 105, 1400–1412. <https://doi.org/10.1111/tpj.15122>.
 52. Wang, Z., Casas-Mollano, J.A., Xu, J., Riethoven, J.-J.M., Zhang, C., and Cerutti, H. (2015). Osmotic stress induces phosphorylation of histone H3 at threonine 3 in pericentromeric regions of Arabidopsis thaliana. *Proc. Natl. Acad. Sci. USA* 112, 8487–8492. <https://doi.org/10.1073/pnas.1423325112>.
 53. Sanagi, M., Lu, Y., Aoyama, S., Morita, Y., Mitsuda, N., Ikeda, M., Ohme-Takagi, M., Sato, T., and Yamaguchi, J. (2018). Sugar-responsive transcription factor bZIP3 affects leaf shape in Arabidopsis plants. *Plant Biotechnol.* 35, 167–170. <https://doi.org/10.5511/plantbiotechnology.18.0410a>.
 54. Posé, D., Castanedo, I., Borsani, O., Nieto, B., Rosado, A., Taconnat, L., Ferrer, A., Dolan, L., Valpuesta, V., and Botella, M.A. (2009). Identification of the Arabidopsis dry2/sqe1-5 mutant reveals a central role for sterols in drought tolerance and regulation of reactive oxygen species. *Plant J.* 59, 63–76. <https://doi.org/10.1111/j.1365-313X.2009.03849.x>.
 55. Li, H., Yu, M., Du, X.-Q., Wang, Z.-F., Wu, W.-H., Quintero, F.J., Jin, X.-H., Li, H.-D., and Wang, Y. (2017). NRT1.5/NPF7.3 Functions as a Proton-Coupled H⁺/K⁺ Antiporter for K⁺ Loading into the Xylem in Arabidopsis. *Plant Cell* 29, 2016–2026. <https://doi.org/10.1105/tpc.16.00972>.
 56. Alassimone, J., Fujita, S., Doblas, V.G., van Dop, M., Barberon, M., Kalmbach, L., Vermeer, J.E.M., Rojas-Murcia, N., Santuari, L., Hardtke, C.S., and Geldner, N. (2016). Polarly localized kinase SGN1 is required for Caspary strip integrity and positioning. *Nat. Plants* 2, 16113. <https://doi.org/10.1038/nplants.2016.113>.
 57. Clay, N.K., and Nelson, T. (2005). The Recessive Epigenetic swellmap Mutation Affects the Expression of Two Step II Splicing Factors Required for the Transcription of the Cell Proliferation Gene STRUWWELPETER and for the Timing of Cell Cycle Arrest in the Arabidopsis Leaf. *Plant Cell* 17, 1994–2008. <https://doi.org/10.1105/tpc.105.032771>.
 58. Inoue, H., Li, M., and Schnell, D.J. (2013). An essential role for chloroplast heat shock protein 90 (Hsp90C) in protein import into chloroplasts. *Proc. Natl. Acad. Sci. USA* 110, 3173–3178. <https://doi.org/10.1073/pnas.1219229110>.
 59. Barragan, C.A., Wu, R., Kim, S.-T., Xi, W., Habring, A., Hagmann, J., Van de Weyer, A.-L., Zaïdem, M., Ho, W.W.H., Wang, G., et al. (2019). RPW8/HR repeats control NLR activation in Arabidopsis thaliana. *PLoS Genet.* 15, e1008313. <https://doi.org/10.1371/journal.pgen.1008313>.
 60. Bulut-Karslioğlu, A. (2024). The double-edged sword of bivalency. *Nat. Rev. Mol. Cell Biol.* 25, 6. <https://doi.org/10.1038/s41580-023-00665-0>.
 61. Braun, S.M.G., Kirkland, J.G., Chory, E.J., Husmann, D., Calarco, J.P., and Crabtree, G.R. (2017). Rapid and reversible epigenome editing by endogenous chromatin regulators. *Nat. Commun.* 8, 560. <https://doi.org/10.1038/s41467-017-00644-y>.
 62. Kadoc, C., Williams, R.T., Calarco, J.P., Miller, E.L., Weber, C.M., Braun, S.M.G., Pulice, J.L., Chory, E.J., and Crabtree, G.R. (2017). Dynamics of BAF-Polycomb complex opposition on heterochromatin in normal and oncogenic states. *Nat. Genet.* 49, 213–222. <https://doi.org/10.1038/ng.3734>.
 63. Dubois, M., Van den Broeck, L., and Inzé, D. (2018). The Pivotal Role of Ethylene in Plant Growth. *Trends Plant Sci.* 23, 311–323. <https://doi.org/10.1016/j.tplants.2018.01.003>.
 64. Binder, B.M. (2020). Ethylene signaling in plants. *J. Biol. Chem.* 295, 7710–7725. <https://doi.org/10.1074/jbc.REV120.010854>.
 65. Schuettengruber, B., Bourbon, H.M., Di Croce, L., and Cavalli, G. (2017). Genome Regulation by Polycomb and Trithorax: 70 Years and Counting. *Cell* 171, 34–57. <https://doi.org/10.1016/j.cell.2017.08.002>.
 66. Kumar, S.V., and Wigge, P.A. (2010). H2A.Z-Containing Nucleosomes Mediate the Thermosensory Response in Arabidopsis. *Cell* 140, 136–147. <https://doi.org/10.1016/j.cell.2009.11.006>.
 67. Sachs, M., Onodera, C., Blaschke, K., Ebata, K.T., Song, J.S., and Ramalho-Santos, M. (2013). Bivalent chromatin marks developmental regulatory genes in the mouse embryonic germline in vivo. *Cell Rep.* 3, 1777–1784. <https://doi.org/10.1016/j.celrep.2013.04.032>.
 68. Matsui, S., Granitto, M., Buckley, M., Ludwig, K., Koigi, S., Shiley, J., Zacharias, W.J., Mayhew, C.N., Lim, H.W., and Iwafuchi, M. (2024). Pioneer and PRDM transcription factors coordinate bivalent epigenetic

- states to safeguard cell fate. *Mol. Cell* 84, 476–489.e10. <https://doi.org/10.1016/j.molcel.2023.12.007>.
69. Zhao, K., Kong, D., Jin, B., Smolke, C.D., and Rhee, S.Y. (2021). A novel bivalent chromatin associates with rapid induction of camalexin biosynthesis genes in response to a pathogen signal in *Arabidopsis*. *eLife* 10, e69508. <https://doi.org/10.7554/eLife.69508>.
 70. Zeng, Z., Zhang, W., Marand, A.P., Zhu, B., Buell, C.R., and Jiang, J. (2019). Cold stress induces enhanced chromatin accessibility and bivalent histone modifications H3K4me3 and H3K27me3 of active genes in potato. *Genome Biol.* 20, 123. <https://doi.org/10.1186/s13059-019-1731-2>.
 71. Wang, H., Yin, C., Zhang, G., Yang, M., Zhu, B., Jiang, J., and Zeng, Z. (2024). Cold-induced deposition of bivalent H3K4me3-H3K27me3 modification and nucleosome depletion in *Arabidopsis*. *Plant J.* 118, 549–564. <https://doi.org/10.1111/tpj.16624>.
 72. Liu, N., Fromm, M., and Avramova, Z. (2014). H3K27me3 and H3K4me3 chromatin environment at super-induced dehydration stress memory genes of *Arabidopsis thaliana*. *Mol. Plant* 7, 502–513. <https://doi.org/10.1093/mp/ssu001>.
 73. Rizzardi, K., Landberg, K., Nilsson, L., Ljung, K., and Sundås-Larsson, A. (2011). TFL2/LHP1 is involved in auxin biosynthesis through positive regulation of YUCCA genes. *Plant J.* 65, 897–906. <https://doi.org/10.1111/j.1365-313X.2010.04470.x>.
 74. Veluchamy, A., Jégu, T., Ariel, F., Latrasse, D., Mariappan, K.G., Kim, S.-K., Crespi, M., Hirt, H., Bergounioux, C., Raynaud, C., and Benhamed, M. (2016). LHP1 Regulates H3K27me3 Spreading and Shapes the Three-Dimensional Conformation of the *Arabidopsis* Genome. *PLoS One* 11, e0158936. <https://doi.org/10.1371/journal.pone.0158936>.
 75. Huq, E., and Quail, P.H. (2002). PIF4, a phytochrome-interacting bHLH factor, functions as a negative regulator of phytochrome B signaling in *Arabidopsis*. *Embo J* 21, 2441–2450. <https://doi.org/10.1093/emboj/21.10.2441>.
 76. Bai, M.Y., Shang, J.X., Oh, E., Fan, M., Bai, Y., Zentella, R., Sun, T.P., and Wang, Z.Y. (2012). Brassinosteroid, gibberellin and phytochrome impinge on a common transcription module in *Arabidopsis*. *Nat. Cell Biol.* 14, 810–817. <https://doi.org/10.1038/ncb2546>.
 77. Bernardo-García, S., de Lucas, M., Martínez, C., Espinosa-Ruiz, A., Davière, J.M., and Prat, S. (2014). BR-dependent phosphorylation modulates PIF4 transcriptional activity and shapes diurnal hypocotyl growth. *Genes Dev.* 28, 1681–1694. <https://doi.org/10.1101/gad.243675.114>.
 78. Vandenbussche, F., Vaseva, I., Vissenberg, K., and Van Der Straeten, D. (2012). Ethylene in vegetative development: a tale with a riddle. *New Phytol.* 194, 895–909. <https://doi.org/10.1111/j.1469-8137.2012.04100.x>.
 79. Lü, P., Yu, S., Zhu, N., Chen, Y.-R., Zhou, B., Pan, Y., Tzeng, D., Fabi, J.P., Argyris, J., Garcia-Mas, J., et al. (2018). Genome encode analyses reveal the basis of convergent evolution of fleshy fruit ripening. *Nat. Plants* 4, 784–791. <https://doi.org/10.1038/s41477-018-0249-z>.
 80. Qiao, H., Shen, Z., Huang, S.S.C., Schmitz, R.J., Urich, M.A., Briggs, S.P., and Ecker, J.R. (2012). Processing and subcellular trafficking of ER-tethered EIN2 control response to ethylene gas. *Science* 338, 390–393. <https://doi.org/10.1126/science.1225974>.
 81. Guo, H., and Ecker, J.R. (2003). Plant responses to ethylene gas are mediated by SCF(EBF1/EBF2)-dependent proteolysis of EIN3 transcription factor. *Cell* 115, 667–677. [https://doi.org/10.1016/s0092-8674\(03\)00969-3](https://doi.org/10.1016/s0092-8674(03)00969-3).
 82. Zong, W., Kim, J., Bordyia, Y., Qiao, H., and Sung, S. (2022). Abscisic acid negatively regulates the Polycomb-mediated H3K27me3 through the PHD-finger protein, VIL1. *New Phytol.* 235, 1057–1069. <https://doi.org/10.1111/nph.18156>.
 83. Wang, L., Zhang, Z., Zhang, F., Shao, Z., Zhao, B., Huang, A., Tran, J., Hernandez, F.V., and Qiao, H. (2021). EIN2-directed histone acetylation requires EIN3-mediated positive feedback regulation in response to ethylene. *Plant Cell* 33, 322–337. <https://doi.org/10.1093/plcell/koaa029>.
 84. Langmead, B., and Salzberg, S.L. (2012). Fast gapped-read alignment with Bowtie 2. *Nat. Methods* 9, 357–359. <https://doi.org/10.1038/nmeth.1923>.
 85. Li, H., Handsaker, B., Wysoker, A., Fennell, T., Ruan, J., Homer, N., Marth, G., Abecasis, G., and Durbin, R.; 1000 Genome Project Data Processing Subgroup (2009). The Sequence Alignment/Map format and SAMtools. *Bioinformatics* 25, 2078–2079. <https://doi.org/10.1093/bioinformatics/btp352>.
 86. Dobin, A., Davis, C.A., Schlesinger, F., Drenkow, J., Zaleski, C., Jha, S., Batut, P., Chaisson, M., and Gingeras, T.R. (2013). STAR: ultrafast universal RNA-seq aligner. *Bioinformatics* 29, 15–21. <https://doi.org/10.1093/bioinformatics/bts635>.
 87. Zhang, Y., Liu, T., Meyer, C.A., Eeckhoute, J., Johnson, D.S., Bernstein, B.E., Nusbaum, C., Myers, R.M., Brown, M., Li, W., and Liu, X.S. (2008). Model-based Analysis of ChIP-Seq (MACS). *Genome Biol.* 9, R137. <https://doi.org/10.1186/gb-2008-9-9-r137>.
 88. Ramírez, F., Dündar, F., Diehl, S., Grüning, B.A., and Manke, T. (2014). deepTools: a flexible platform for exploring deep-sequencing data. *Nucleic Acids Res.* 42, W187–W191. <https://doi.org/10.1093/nar/gku365>.
 89. Liao, Y., Smyth, G.K., and Shi, W. (2013). The Subread aligner: fast, accurate and scalable read mapping by seed-and-vote. *Nucleic Acids Res.* 41, e108. <https://doi.org/10.1093/nar/gkt214>.
 90. Love, M.I., Huber, W., and Anders, S. (2014). Moderated estimation of fold change and dispersion for RNA-seq data with DESeq2. *Genome Biol.* 15, 550. <https://doi.org/10.1186/s13059-014-0550-8>.
 91. Yu, G., Wang, L.G., and He, Q.Y. (2015). ChIPseeker: an R/Bioconductor package for ChIP peak annotation, comparison and visualization. *Bioinformatics* 31, 2382–2383. <https://doi.org/10.1093/bioinformatics/btv145>.
 92. Schindelin, J., Arganda-Carreras, I., Frise, E., Kaynig, V., Longair, M., Pietzsch, T., Preibisch, S., Rueden, C., Saalfeld, S., Schmid, B., et al. (2012). Fiji: an open-source platform for biological-image analysis. *Nat. Methods* 9, 676–682. <https://doi.org/10.1038/nmeth.2019>.
 93. Tian, T., Liu, Y., Yan, H., You, Q., Yi, X., Du, Z., Xu, W., and Su, Z. (2017). agriGO v2.0: a GO analysis toolkit for the agricultural community, 2017 update. *Nucleic Acids Res.* 45, W122–W129. <https://doi.org/10.1093/nar/gkx382>.
 94. Shao, Z., Zhao, B., Kotla, P., Burns, J.G., Tran, J., Ke, M., Chen, X., Browning, K.S., and Qiao, H. (2022). Phosphorylation status of B β sub-unit acts as a switch to regulate the function of phosphatase PP2A in ethylene-mediated root growth inhibition. *New Phytol.* 236, 1762–1778. <https://doi.org/10.1111/nph.18467>.
 95. Zhao, B., Wang, L., Shao, Z., Chin, K., Chakravarty, D., and Qiao, H. (2021). ENAP1 retrains seed germination via H3K9 acetylation mediated positive feedback regulation of ABI5. *PLoS Genet.* 17, e1009955. <https://doi.org/10.1371/journal.pgen.1009955>.
 96. Zhao, B., Shao, Z., Wang, L., Zhang, F., Chakravarty, D., Zong, W., Dong, J., Song, L., and Qiao, H. (2022). MYB44-ENAP1/2 restricts HDT4 to regulate drought tolerance in *Arabidopsis*. *PLoS Genet.* 18, e1010473. <https://doi.org/10.1371/journal.pgen.1010473>.
 97. Shao, Z., Bian, L., Ahmadi, S.K., Daniel, T.J., Belmonte, M.A., Burns, J.G., Kotla, P., Bi, Y., Shen, Z., Xu, S.L., et al. (2024). Nuclear Pyruvate Dehydrogenase Complex Regulates Histone Acetylation and Transcriptional Regulation in the Ethylene Response. *bioRxiv*. <https://doi.org/10.1101/2023.10.25.564010>.
 98. Chen, C.Y., Shao, Z., Wang, G., Zhao, B., Hardtke, H.A., Leong, J., Zhou, T., Zhang, Y.J., and Qiao, H. (2024). Histone acetyltransferase HAF2 associates with PDC to control H3K14ac and H3K23ac in ethylene response. *bioRxiv*. <https://doi.org/10.1101/2023.12.31.573642>.

99. Luo, X., Gao, Z., Wang, Y., Chen, Z., Zhang, W., Huang, J., Yu, H., and He, Y. (2018). The NUCLEAR FACTOR-CONSTANS complex antagonizes Polycomb repression to de-repress FLOWERING LOCUS T expression in response to inductive long days in Arabidopsis. *Plant J.* **95**, 17–29. <https://doi.org/10.1111/tpj.13926>.
100. Zhong, S., Zhao, M., Shi, T., Shi, H., An, F., Zhao, Q., and Guo, H. (2009). EIN3/EIL1 cooperate with PIF1 to prevent photo-oxidation and to promote greening of *Arabidopsis* seedlings. *Proc. Natl. Acad. Sci. USA* **106**, 21431–21436. <https://doi.org/10.1073/pnas.0907670106>.
101. Zhang, F., Wang, L., Qi, B., Zhao, B., Ko, E.E., Riggan, N.D., Chin, K., and Qiao, H. (2017). EIN2 mediates direct regulation of histone acetylation in the ethylene response. *Proc. Natl. Acad. Sci. USA* **114**, 10274–10279. <https://doi.org/10.1073/pnas.1707937114>.
102. Desvoyes, B., Sequeira-Mendes, J., Vergara, Z., Madeira, S., and Gutierrez, C. (2018). Sequential ChIP Protocol for Profiling Bivalent Epigenetic Modifications (ReChIP). *Methods Mol. Biol.* **1675**, 83–97. https://doi.org/10.1007/978-1-4939-7318-7_6.

STAR★METHODS

KEY RESOURCES TABLE

REAGENT or RESOURCE	SOURCE	IDENTIFIER
Antibodies		
Mouse monoclonal anti-HA	Biolegend	Cat# 901503; RRID: AB_2565005
Rabbit monoclonal anti-FLAG	Cell Signaling Technology	Cat#14793; RRID: AB_2572291
Rabbit polyclonal anti-GFP	Invitrogen	Cat#A-11122; RRID: AB_221569
Rabbit polyclonal anti-EIN2	Qiao et al. ⁸⁰	N/A
Rabbit polyclonal anti-EIN3	Guo et al. ⁸¹	N/A
Rabbit polyclonal Histone anti-H3K4me3	Active Motif	Cat# 39016; RRID: AB_2687512
Mouse monoclonal Histone anti-H3K27me3	Active Motif	Cat# 61017; RRID: AB_2614987
Mouse monoclonal GAL4-TA Antibody	Santa Cruz Biotechnology	Cat# sc-46680; RRID: AB_669109
Mouse monoclonal GAL4 [DBD] Antibody	Santa Cruz Biotechnology	Cat# sc-510; RRID: AB_627655
Goat polyclonal anti Mouse Kappa Light Chain	Bio-Rad	Cat#105001; RRID: AB_618653
Goat polyclonal anti-Rabbit IgG (H + L)-HRP Conjugate	Bio-Rad	Cat#170–6515; RRID: AB_11125142
Bacterial and virus strains		
<i>Agrobacterium tumefaciens</i> , strain GV3101	N/A	N/A
<i>Escherichia coli</i> (<i>E. coli</i>), strain Top10	N/A	N/A
Deposited data		
RNA-seq data	This study	GEO: GSE256453
Experimental models: organisms/strains		
<i>Arabidopsis</i> : <i>ein2-5</i>	Qiao et al. ⁸⁰	N/A
<i>Arabidopsis</i> : <i>ein3-1 eil1-1</i>	Qiao et al. ⁸⁰	N/A
<i>Arabidopsis</i> : <i>lhp1-3</i>	Zong et al. ⁸²	N/A
<i>Arabidopsis</i> : <i>ein2-5 lhp1-3</i>	This study	N/A
<i>Arabidopsis</i> : <i>ein3-1 eil1-1 lhp1-3</i>	This study	N/A
<i>Arabidopsis</i> : <i>pif4-2</i>	Lee et al. ¹⁰	N/A
<i>Arabidopsis</i> : <i>proLHP1::gLHP1-GFP/lhp1-6 FRI</i>	Yang et al. ³³	N/A
<i>Arabidopsis</i> : <i>proLHP1::gLHP1-GFP/lhp1-6</i>	This study	N/A
<i>Arabidopsis</i> : <i>proLHP1::gLHP1-GFP/ein2-5 lhp1-6</i>	This study	N/A
<i>Arabidopsis</i> : <i>proLHP1::gLHP1-GFP/ein3-1 eil1-1 lhp1-6</i>	This study	N/A
<i>Arabidopsis</i> : <i>ein2-5 lhp1-6</i>	This study	N/A
<i>Arabidopsis</i> : <i>ein3-1 eil1-1 lhp1-6</i>	This study	N/A
<i>Arabidopsis</i> : <i>35S::LHP1-FLAG-BFP/EIN2^{S645A}-YFP-HA</i>	This study	N/A
<i>Arabidopsis</i> : <i>ino80-5</i>	Xue et al. ²⁴	N/A
<i>Arabidopsis</i> : <i>ein2-5 ino80-5</i>	This study	N/A
<i>Arabidopsis</i> : <i>ein3-1 eil1-1 ino80-5</i>	This study	N/A
<i>Arabidopsis</i> : <i>lhp1-3 ino80-5</i>	This study	N/A
<i>Arabidopsis</i> : <i>35S::HA-INO80/ino80-5</i>	Xue et al. ²⁴	N/A
<i>Arabidopsis</i> : <i>35S::HA-INO80/ein2-5 ino80-5</i>	This study	N/A
<i>Arabidopsis</i> : <i>35S::HA-INO80/ein3-1 eil1-1 ino80-5</i>	This study	N/A
<i>Arabidopsis</i> : <i>35S::HA-INO80/lhp1-3 ino80-5</i>	This study	N/A
<i>Arabidopsis</i> : <i>35S::HA-INO80/EIN3ox</i>	This study	N/A
Oligonucleotides		
Primers used in this study are listed in Table S1	This study	N/A
Recombinant DNA		
<i>pEXPAD502-LHP1</i>	This study	N/A

(Continued on next page)

Continued

REAGENT or RESOURCE	SOURCE	IDENTIFIER
pDBLeu-LHP1	This study	N/A
pEXPAD502-EIN3	Wang et al. ⁸³	N/A
pDBLeu-EIN2-C	Wang et al. ⁸³	N/A
pEXPAD502-INO80-N	This study	N/A
pDBLeu-INO80-N	This study	N/A
pEXPAD502-INO80-C	This study	N/A
pDBLeu-INO80-C	This study	N/A
pGEX-KG-GST-LHP1	This study	N/A
pGEX-KG-GST-INO80-N	This study	N/A
pCambia1300-LHP1-FLAG-BFP	This study	N/A
Software and algorithms		
FastQC	Babraham Institute	N/A
Trim Galore	Babraham Institute	N/A
Bowtie 2 (2.4.2)	Langmead et al. ⁸⁴	N/A
SAMtools	Li et al. ⁸⁵	N/A
STAR	Dobin et al. ⁸⁶	N/A
MACS2	Zhang et al. ⁸⁷	N/A
deeptools3.0.2	Ramírez et al. ⁸⁸	N/A
Subread 2.0.1	Liao et al. ⁸⁹	N/A
DESeq2	Love et al. ⁹⁰	N/A
ChIPseeker	Yu et al. ⁹¹	N/A

EXPERIMENTAL MODEL AND STUDY PARTICIPANT DETAILS

All *Arabidopsis thaliana* plants used in this study were in the Col-0 ecotype background and grown at continuous temperatures of 21°C or 27°C in the growth chamber set with same light intensity condition and an 8-h-light/16-h-dark short-day (SD) light cycle. The phenotypic assays in response to warm ambient temperature were performed according to previous publication.²⁷ In brief, approximately 50 seeds of each genotype collected at the similar time were surface sterilized, plated on the same Murashige & Skoog (MS) medium supplemented with 1% sucrose, and placed at 4°C in the dark for three days for stratification. After germination was induced at 21°C for 24 h, seedlings were either shifted to 27°C SD conditions or kept at 21°C SD as control till day 5. Their hypocotyl lengths were measured using Fiji ImageJ software.⁹² The mutants *ein2-5*, *ein3-1 eil1-1*, *lhp1-3*, *lhp1-6*, *ino80-5*, and *pif4-2* were used in this study. Higher order mutants were generated by genetic crossing. *EIN2*, *EIN3*, *LHP1*, and *INO80* related transgenic plants were derived from previous publications,^{24,33,80,81} except 35S::LHP1-FLAG-BFP/Col-0 (generated in this study). To obtain *proLHP1::gLHP1-GFP/lhp1-6*, *proLHP1::gLHP1-GFP/ein2-5 lhp1-6*, and *proLHP1::gLHP1-GFP/ein3-1 eil1-1 lhp1-6* complementation lines, *proLHP1::gLHP1-GFP/lhp1-6 FRI* was backcrossed to Col-0, *ein2-5*, and *ein3-1 eil1-1* to remove *FRI*, respectively; *lhp1-6*, *ein2-5 lhp1-6*, and *ein3-1 eil1-1 lhp1-6* were also generated from the same crossed population by segregation. Homozygous plants of both *proLHP1::gLHP1-GFP* transgene and related gene null mutations with comparable *gLHP1-GFP* expression levels were used for following analyses. The 35S::HA-INO80/*ein2-5 ino80-5*, 35S::HA-INO80/*ein3-1 eil1-1 ino80-5*, and 35S::HA-INO80/*lhp1-3 ino80-5* lines were generated by genetic crossing 35S::HA-INO80/*ein2-5 ino80-5* with *ein2-5*, *ein3-1 eil1-1*, and *lhp1-3*, respectively.

METHOD DETAILS

Plant protein extraction and western blot assays

To assess warm ambient temperature response at the protein level, seedlings in each indicated genetic background after warm ambient temperature treatment were frozen and homogenized in liquid nitrogen. Total protein was extracted with extraction buffer (100 mM Tris-HCl, pH 7.5, 100 mM NaCl, 5 mM EDTA, 5 mM DTT, 10 mM β-mercaptoethanol, 1% SDS, 1 mM PMSF, and 1X protease inhibitors from Thermo Fisher), and the plant debris was removed by centrifugation. The extracted proteins in the supernatant were further denatured at 85°C for 5 min after mixing with 2x Laemmli sample buffer and subject to SDS-PAGE. The protein levels were detected by immunoblot analysis using the primary antibodies: anti-HA antibody (Biolegend, #901503, dilution 1:5000), anti-FLAG antibody (CST, #14793, dilution 1:2000), anti-EIN2 antibody (raised in-house, dilution 1:2000),⁸⁰ anti-EIN3 antibody (raised in-house, dilution 1:2000),⁸¹ anti-GFP antibody (Invitrogen, A11122, dilution 1:2000), and anti-PIF4 (Agrisera, AS16 3955, dilution 1:2000) and

corresponding secondary antibodies: anti-mouse (Bio-Rad, #105001G, dilution 1:10000), anti-rabbit (Bio-Rad, #1706515, dilution 1:10000), and anti-goat (Agrisera, AS09 605, dilution 1:5000). HRP activity was detected using enhanced chemiluminescence (ECL; GE Healthcare) according to the manufacturer's instructions with either ChemiDoc Imaging System (Bio-Rad) or conventional X-ray films.

Plant RNA extraction and gene expression analysis

To assess transcriptional response to warm ambient temperature treatment, five-day-old green seedlings in each indicated genetic background grown in 21°C SD were shifted to warm ambient temperature (27°C) from ZT4 for 4 h till ZT8 in SD condition or kept at 21°C till ZT8. Plants samples were collected at 21°C 0h (ZT4 21°C, before treatment), 27°C 4h (ZT8 27°C, warm ambient temperature treatment), and 21°C 4h (ZT8 21°C, control treatment) and immediately snap-frozen in liquid nitrogen. Total RNA was extracted after frozen seedlings were homogenized in liquid nitrogen using the RNeasy Plant Kit (Qiagen) with DNase I digestion and clean up (Qiagen, RNeasy Mini Kit (250)). First-strand cDNA was synthesized using Invitrogen Superscript III First-Strand cDNA Synthesis Kit. cDNAs and qPCR primers were combined with 2X SYBR master mix from Thermo Fisher for qPCR. PCR reactions were performed in triplicates on a Roche 96 Thermal cycler. *ACTIN2* was used as endogenous control for normalization. Three independent biological replicates were performed with reproducible results. Primers used in this study are listed in [Table S1](#).

mRNA sequencing and data processing

RNA was extracted from five-day-old green seedlings with or without 4 h of 27°C treatment of each genotype using the RNeasy Plant Kit (Qiagen). For mRNA sequencing (mRNA-seq) library preparations, libraries were generated using the NEBNext Poly(A) mRNA Magnetic Isolation Module (E7490) and the NEBNext Ultra II RNA Library Prep Kit for Illumina (E7770), with 1 µg RNA as input, following the manufacturer's instructions. Indexed libraries were sequenced on the platform of HiSeq2000 (Illumina). Paired-end raw fastq data were evaluated with FastQC and low-quality reads were removed with Trim Galore (Babraham Institute). The trimmed and filtered reads were then mapped to the *Arabidopsis* reference genome (TAIR10) with STAR.⁸⁶ Mapped reads were counted by featureCounts (Subread 2.0.1) and differentially regulated genes were identified using R package DESeq2⁹⁰ with a p-adj < 0.05 and |log2(fold change)| > 0.585 (|fold change| > 1.5). The boxplots, violin plots, and dot plots were generated by R package ggplot2 and the heatmaps of log2FC were generated by R package pheatmap. GO enrichment analysis for DEGs was performed by agriGO v2.⁹³ Trimmed and aligned read counts are listed in [Table S2](#).

Yeast two-hybrid assay

The yeast two-hybrid assay was performed according to previous publications using the ProQuest Two-Hybrid System (Invitrogen) following the manufacturer's instructions.^{94,95} Briefly, the bait and prey plasmids (pAD-LHP1, pBD-LHP1, pAD-EIN3, pBD-EIN2-C, pAD-INO80-N, pBD-INO80-N, pAD-INO80-C, and pBD-INO80-C) were co-transformed into the yeast strain AH109, following the experiment design. For INO80 related Y2H assays, INO80 full length protein was truncated to INO80-N (1-500aa) and INO80-C (501-1540aa) for optimal expression in yeast according to literature.²⁴ The positive transformants were selected and grown on SD/-Leu-Trp (two-dropout) medium. 3-amino-1,2,4-triazole (3-AT) was supplemented to repress self-activation. Growth on SD/-Leu-Trp-His (three-dropout) medium supplemented with appropriate concentrations of 3-AT indicates the physical interaction between corresponding proteins.

Transient expression in *Nicotiana benthamiana* leaves

To co-express EIN2-C-YFP-HA and LHP1-FLAG-BFP fusion proteins in *N. benthamiana* for pull-down assays, 20 mL overnight cultures of *Agrobacterium tumefaciens* (strain GV3101) in LB medium carrying the 35S::EIN2-C-YFP-HA pEarleyGate101 and 35S::LHP1-FLAG-BFP pCambia1300 binary vectors respectively were pelleted by centrifuge at 2000 g at room temperature for 15 min and then resuspended in infiltration buffer (10 mM MgCl₂, 10 mM MES, pH 5.7, and 100 µM acetosyringone, AS). Paired re-suspended Agrobacterium cultures were combined and then mixed with an equal volume of p19 agrobacteria resuspension to reach a final OD600 of 0.8 for each resuspension before the infiltration at the abaxial side of *N. benthamiana* leaves using a needless syringe. After growth for 48–72 h under dim light condition, infected tobacco leaves were collected and snap frozen in LN2 for further protein analysis.

Co-immunoprecipitation

Co-immunoprecipitation (Co-IP) assays between proteins of interest were performed according to previous publications.^{96,97} In brief, soluble total proteins were extracted from fine ground plant tissues in two volumes of co-IP buffer (50 mM Tris-Cl, pH 8, 150 mM NaCl, 1 mM EDTA, 0.1% Triton X-100, 1 mM PMSF, and 1x protease inhibitor cocktail) at 4°C for 15 min with gentle rocking. The lysates were cleared by centrifugation at 4°C (10 min, 5000 g). For HA-INO80 fusion protein related co-IP experiments, the anti-HA antibody (Biolegend, #901503) was prebound to the equilibrated IgG coated Dynabeads (Thermo Fisher) for 3 h with gentle rotation at 4°C. For LHP1-FLAG-BFP fusion protein related co-IP assays, DYKDDDDK Fab-Trap agarose beads (ChromoTek) were used to immunoprecipitate LHP1 protein complexes, following the same procedure. A 10% input aliquot for each co-IP experiment was taken from the cleared supernatant before the rest of the supernatant was added to magnetic beads and incubated at 4°C with gentle rocking overnight. IgG coated Dynabeads were incubated with protein extracts as negative control for anti-HA IP experiment, while

protein extracts containing prey protein alone were incubated with DYKDDDDK Fab-Trap agarose beads to serve as negative controls. Magnetic beads with IP products were precipitated magnetically using a DynaMagnetic rack (Thermo Fisher) and then washed five times with 1 mL of co-IP buffer. Immunoprecipitated proteins were then released from the magnetic beads using 2x Laemmli sample buffer by heating at 85°C for 8 min and subject to SDS-PAGE.

ChIP sequencing data analysis

Publicly available ChIP sequencing (ChIP-seq) datasets of LHP1, H3K27me3, and H3K4me3 were obtained from the Gene Expression Omnibus (GEO) database.^{39,43,49} Raw sequencing data were subject to quality control by FastQC. Low quality reads were removed with Trim Galore (Babraham Institute) and then mapped to the Arabidopsis genome with Bowtie 2 (2.4.2).⁸⁴ Duplicate reads were removed using SAMtools and broad peak calling for methylated H3 was performed using MACS2 with ‘–broad’ option.⁸⁷ Histone modification peaks were assigned to corresponding genes if a peak overlaps with the proximal region of a gene, including 1.5 kb upstream of TSS and 1.5 kb downstream of TES, by ChIPseeker.⁹¹ ChIP-seq coverage tracks shown in the genome browser IGV were generated using the bamCoverage function in deeptools3.0.2⁸⁸ normalized by reads per genomic content (1x normalization, 1X RPGC) and bin size = 1. The ChIP-seq signals from 2kb upstream TSS to 2kb downstream TES of indicated warm ambient temperature related DEG groups were calculated with bamCompare and computeMatrix and plotted with plotProfile function in deepTools.

ChIP-qPCR assays

Chromatin immunoprecipitation was performed according to previous publications.^{83,98} In brief, five-day-old green seedlings shifted to 27°C for 4 h or kept at 21°C were harvested at the same time (ZT8, SD) and crosslinked in 1% formaldehyde. For EIIN3 and LHP1 related ChIP-qPCR assays, plant samples prior to the 4-h treatment were also collected at 21°C ZT4 (21°C, 0h) as EIIN3 and LHP1 are reported to be regulated by light cycle and circadian clock.^{99,100} For EIN2-C ChIP assays, the long-arm crosslinker, ethylene glycol bis-(succinimidyl succinate) (EGS), was used for fixation according to previous publication.¹⁰¹ Nuclei were isolated and the chromatin was sheared by Bioruptor to approximate 200–300 bp fragments. Anti-GFP (Invitrogen, A11122, for LHP1 binding), anti-EIIN3, anti-EIN2, anti-H3K27me3 (Active Motif, 61017), anti-H3K4me3 (Active Motif, 39016), or anti-HA (Biolegend, #901503, for INO80 binding) antibodies together with Dynabeads were added to the sonicated chromatin followed by incubation overnight in 4°C to precipitate protein bound DNA fragments. The sequential ChIP (Re-ChIP) assays were performed according to previous publications.^{48,101,102} In brief, the first round of ChIP was performed following the same procedure as described using anti-H3K4me3. ChIP chromatin fragments from first round of ChIP assay (IP1: H3K4me3) were recovered in elution buffer (50 mM Tris-HCl pH = 8.0, 5 mM EDTA, 20 mM DTT, and 1% SDS). After desalting and detergent removal, the eluted IP1 chromatin fragments were equally split for second round of IPs against anti-H3K4me3, anti-H3K27me3, and no addition of antibody (IgG as negative control), respectively. The amount of immunoprecipitated DNA was quantified by qPCR and normalized to input DNA. Three independent biological replicates were performed for each line and condition with reproducible results. Primers used for ChIP-qPCR are listed in Table S1.

QUANTIFICATION AND STATISTICAL ANALYSIS

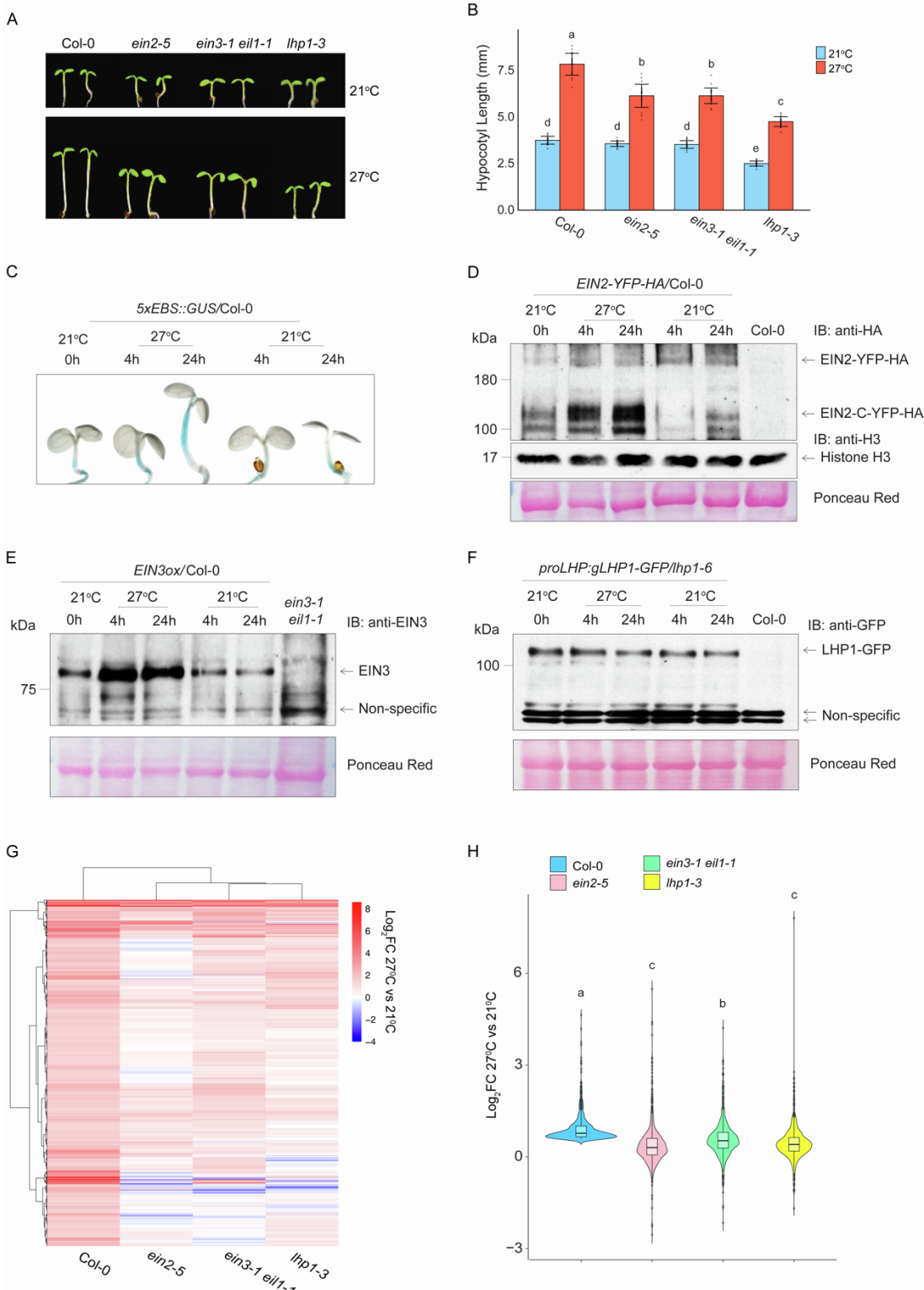
Statistical analyses were performed in R studio except for the transcriptomic analyses, which are explained in their corresponding sections. Number of biological replicates and statistical tests applied are indicated in the figure legends. Numerical *p* values are either indicated in the figures or compact letter display was used for multiple testing. *p* values ≤ 0.05 were considered statistically significant. Individual comparisons between the means of different samples were assessed with two-tailed t test (two samples); One-way ANOVA test followed by Tukey’s HSD test were used if more than two samples.

Supplemental information

**LHP1 and INO80 cooperate with ethylene signaling
for warm ambient temperature response
by activating specific bivalent genes**

Zhengyao Shao, Yanan Bai, Enamul Huq, and Hong Qiao

1 Supplemental Materials



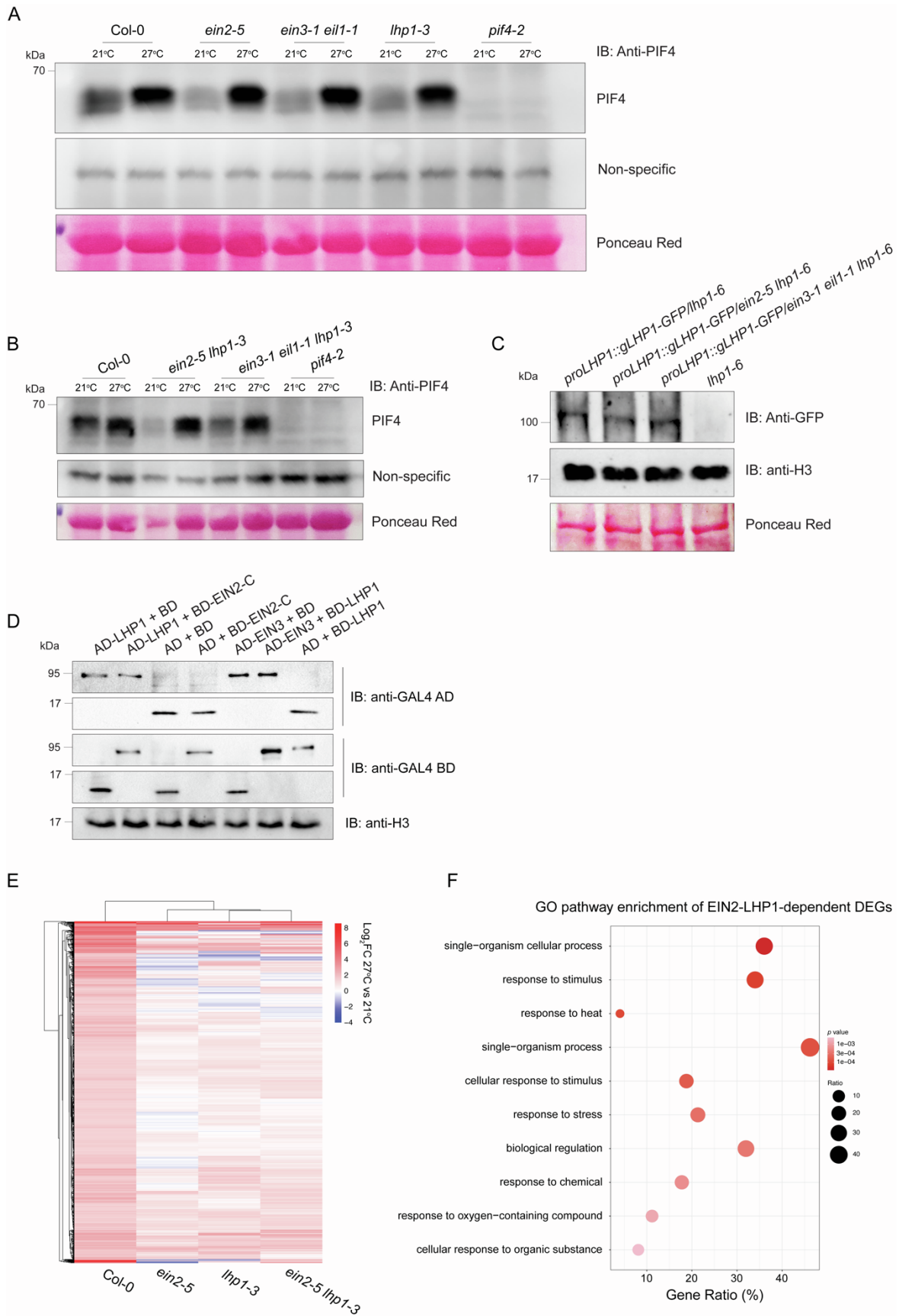
3 **Supplemental Figure 1. Supporting Figure 1. EIN2, EIN3, and LHP1 are required for**
4 **warm ambient temperature response.**

5 **(A)** Representative images of five-day-old green seedlings of Col-0, *ein2-5*, *ein3-1 eil1-1*,
6 and *lhp1-3* grown on MS medium at either 21°C or 27°C. **(B)** Measurements of hypocotyl
7 lengths of indicated mutants in **(A)**. Values are means ± SD of at least 30 seedlings.
8 Different letters represent significant differences between each genotype calculated by a
9 One-way ANOVA test followed by Tukey's HSD test with $P \leq 0.05$. **(C)** β-glucuronidase
10 (GUS) staining to show the warm ambient temperature induced EIN3 transcriptional
11 activity in 5xEBS::GUS/Col-0 transgenic plants. Five-day-old green seedlings were
12 collected at indicated time points and temperature condition and subsequently subject to
13 GUS staining. **(D)** Western blot assay to examine EIN2-C protein levels under warm
14 ambient temperature condition (27°C). Five-day-old green seedlings of *EIN2-YFP-*
15 *HA/Col-0* were used for warm ambient temperature treatment and Col-0 seedlings were
16 used as negative control. Anti-HA antibody was used to detect full-length EIN2-YFP-HA
17 and cleavage product EIN2-C-YFP-HA proteins and anti-H3 antibody was used to detect
18 histone H3 as loading control. **(E)** Western blot assay to detect EIN3 protein levels with
19 warm ambient temperature treatment. Total protein extracts from five-day-old green
20 seedlings of indicated plants with or without warm ambient temperature treatment were
21 subjected to immunoblots against anti-EIN3 antibody. The total protein extracts from *ein3-*
22 *1 eil1-1* seedlings served as negative controls. **(F)** Western blot assay to examine LHP1
23 protein levels under warm ambient temperature condition (27°C). Total protein extracts
24 from five-day-old green seedlings of indicated plants with or without warm ambient
25 temperature treatment were subjected to immunoblotting against anti-GFP antibody.

26 Primary antibody cross-reactive non-specific bands from immunoblots were used to
27 indicate protein loading amounts in (**E-F**). Ponceau red staining of Rubisco was used as
28 an additional internal loading control (lower panels) in (**D-F**). (**G**) Heatmap representation
29 of $\log_2(\text{Fold Change } 27^\circ\text{C vs } 21^\circ\text{C})$ of warm ambient temperature activated differential
30 expressed genes identified in Col-0 in Col-0, *ein2-5*, *ein3-1 eil1-1*, and *lhp1-3* mutant
31 backgrounds. (**H**) Violin plot of the distributions of $\log_2(\text{Fold Change } 27^\circ\text{C vs } 21^\circ\text{C})$ of
32 warm ambient temperature up-regulated genes in Col-0 and in the indicated mutant plants.
33 *P* values were determined by a two-tailed *t* test and different letters represent statistically
34 significant difference (*P* value < 0.05).

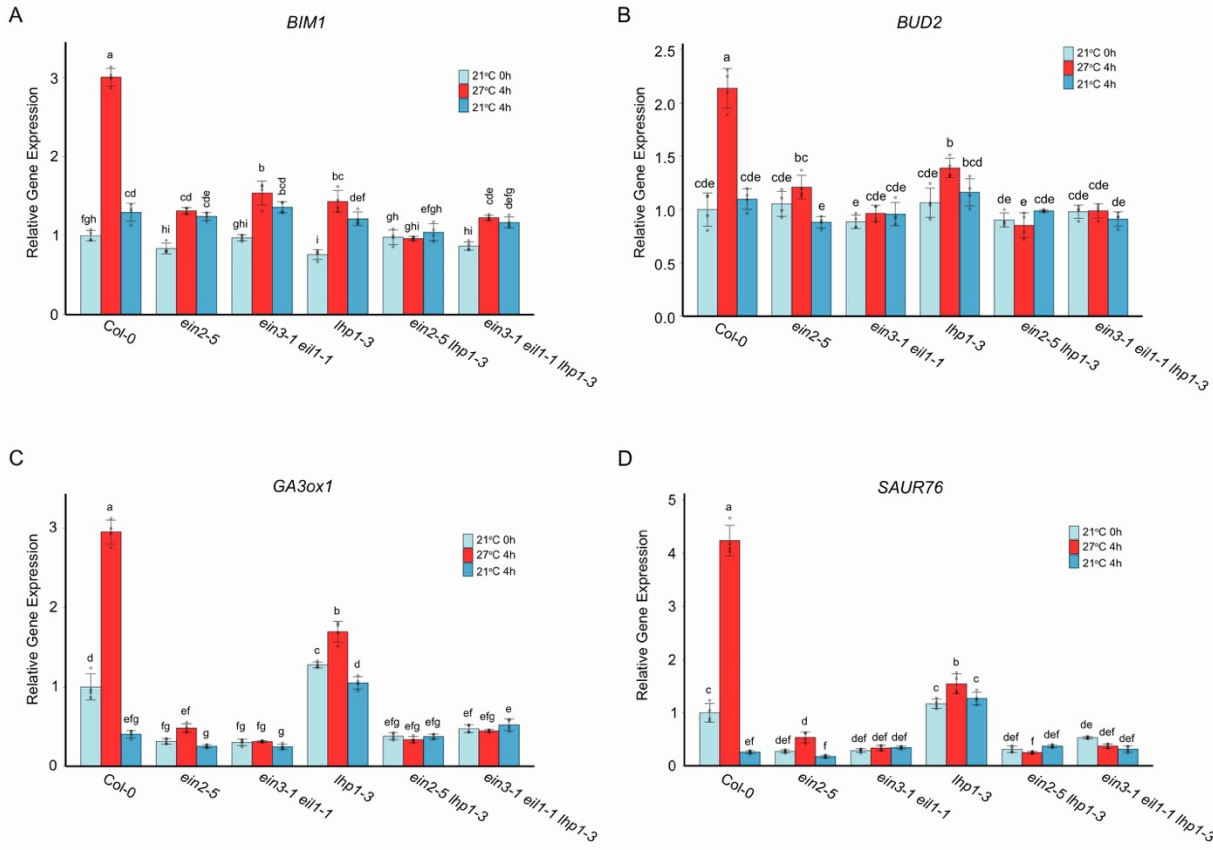
35

36



38 **Supplemental Figure 2. Supporting Figure 1 and 2. EIN2 and LHP1 cofunction in**
39 **warm ambient temperature response at transcriptional level.**

40 (**A** and **B**) Immunoblot assays to examine PIF4 protein levels under warm ambient
41 temperature treatment in various genetic backgrounds. Anti-PIF4 antibody was used to
42 detect endogenous PIF4 proteins in the indicated five-day-old green seedlings with or
43 without warm ambient temperature treatment. Total protein extracts from *pif4-2* mutant
44 seedlings served as negative controls. Ponceau red staining of Rubisco proteins (lower
45 panel) and a non-specific band (middle panel) served as internal loading controls. (**C**)
46 Western blot assay to examine LHP1 protein levels in the complementation transgenic
47 lines of *proLHP1::gLHP1-GFP/lhp1-6*, *proLHP1::gLHP1-GFP/ein2-5 lhp1-6*, and
48 *proLHP1::gLHP1-GFP/ein3-1 eil1-1 lhp1-6*. Five-day-old green seedlings were collected,
49 and *lhp1-6* was used as negative control in the anti-GFP immunoblot. Anti-H3 immunoblot
50 (middle panel) and ponceau red staining (lower panel) were used as loading controls. (**D**)
51 Western blot assays to examine the protein expression levels in yeast strains that contain
52 different plasmids as indicated in the figure. (**E**) Heatmap to compare genes that are up-
53 regulated by warm ambient temperature treatment in Col-0 but their transcriptional
54 activation is reduced in the indicated mutant plants. (**F**) Gene ontology analysis of those
55 warm ambient temperature-induced genes that are further transcriptionally co-
56 compromised in *ein2-5 lhp1-3* double mutant compared to those in *ein2-5* and *lhp1-3*
57 single mutants identified in Fig. 2A. Top 10 GO categories ranked by *P* values were plotted.
58 Dot size represents the percentage of genes from each GO category of total EIN2-LHP1-
59 dependent genes (Gene ratio %) and dot colors indicate the *P* value of the GO categories.



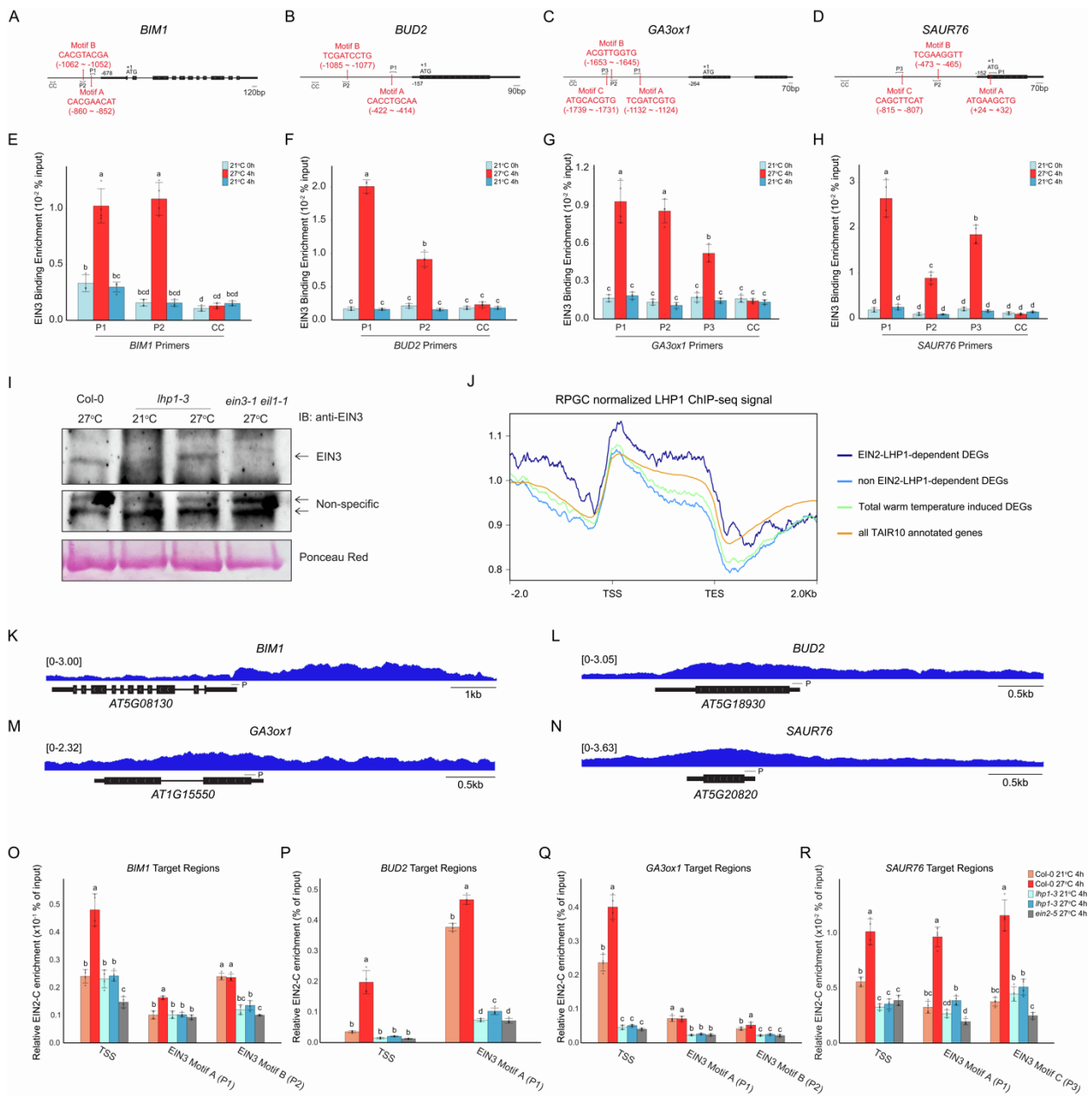
61

62 **Supplemental Figure 3. Supporting Figure 2. EIN2, EIN3, and LHP1 collectively 63 contribute to warm ambient temperature induced transcriptional activation.**

64 (A-D) qRT-PCR analyses of target gene expressions in *Col-0*, *ein2-5*, *ein3-1 eil1-1*, *lhp1-3*, *ein2-5 lhp1-3*, and *ein3-1 eil1-1 lhp1-3* five-day-old green seedlings prior to the warm ambient temperature treatment (21°C 0h) and with or without the following four hours of 27°C treatment (27°C 4h and 21°C 4h, respectively). Values are average of relative expression from each gene normalized to that of *Actin2*. Error bar indicates the SD (n = 4) and different letters indicate statistically significant differences (One-way ANOVA test followed by Tukey's HSD test, $P \leq 0.05$).

71

72



73

74 Supplemental Figure 4. Supporting Figure 2. EIN3 and LHP1 bind to EIN2-LHP1- 75 dependent warm ambient temperature induced target genes.

76 (A-D) Gene models of *BIM1*, *BUD2*, *GA3ox1*, and *SAUR76* loci. The red vertical bars
77 indicate putative EIN3 binding motifs. Locations relative to ATG and DNA sequences of
78 each identified EIN3 binding motifs are labeled, respectively. Black bracelets indicate
79 qPCR amplicons in EIN3 binding ChIP-qPCR assays. P1 (primer 1), P2 (primer 2), and

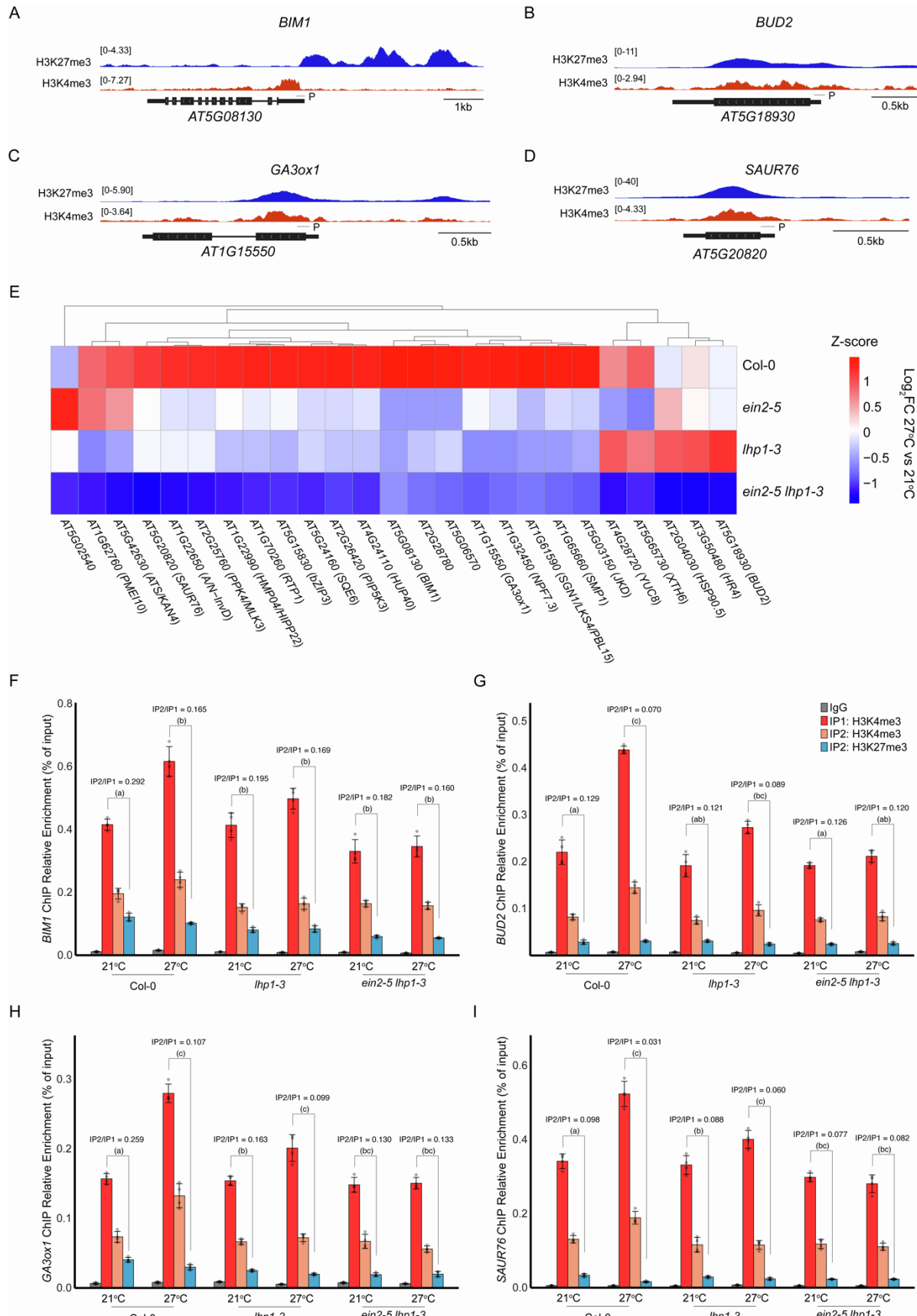
80 P3 (primer 3) represent the qPCR amplicons targeting motif A, motif B, and motif C in
81 each gene (if any), respectively. Negative control (CC) amplicon primers were designed
82 at least 500bp upstream of its closest EIN3 binding motif. (E-H) ChIP assay to examine
83 the relative enrichments of EIN3 binding in Col-0 around EIN3 binding motifs in targeted
84 gene loci. The ChIP assay used anti-EIN3 antibody on green seedlings grown for five
85 days at 21°C in SD with or without warm ambient temperature treatment. The
86 immunoprecipitated DNA fragments were relatively normalized to input. P1, P2, and P3
87 indicate the ChIP-qPCR amplicons of each EIN3 binding motifs illustrated in (A-D),
88 respectively. Negative control (CC) amplicons were used to show the specificity of EIN3
89 ChIP enrichment by anti-EIN3. P1 (Motif A) and P2 (Motif B) for *BIM1*, P1 (Motif A) for
90 *BUD2*, P1 (Motif A) and P2 (Motif B) for *GA3ox1*, and P1 (Motif A) and P3 (Motif C) for
91 *SAUR76* were used for the following binding analyses as those motif regions show higher
92 EIN3 binding affinity. Error bars: \pm S.D., n= 4. Different letters indicate statistical difference
93 in a One-way ANOVA test followed by Tukey's HSD test, $P \leq 0.05$. (I) Western blot assay
94 to examine endogenous EIN3 protein levels in Col-0 and *lhp1-3* mutant with or without
95 warm ambient temperature treatment. Total protein extracts from five-day-old green
96 seedlings were subjected to anti-EIN3 antibody. The total protein extracts from *ein3-1*
97 *eil1-1* mutant seedlings served as negative controls. Non-specific bands from the
98 immunoblots (middle panel) and ponceau red staining of Rubisco proteins (lower panel)
99 served as an internal loading control. (J) Profile plot demonstrating that LHP1
100 preferentially binds to the EIN2-LHP1-dependent warm ambient temperature activated
101 genes. LHP1 ChIP-seq signals from the regions between 2 kb upstream of Transcription
102 Start Sites (TSS) and 2 kb downstream of Transcription End Site (TES) surrounding the

103 gene body were plotted as indicated in the figure. (**K-N**) IGV genome browser snapshots
104 of LHP1 binding in target genes. Horizontal lines represent the amplicons of LHP1 ChIP-
105 qPCR and P represents ChIP-qPCR primer used in Fig. 2H-2K. (**O-R**) ChIP-qPCR assays
106 to examine the relative enrichments of EIN2-C binding in the indicated plants at the
107 selected target gene loci. The ChIP assay was performed using anti-EIN2 antibody with
108 the long-arm crosslinker on green seedlings grown for five days at 21°C in SD with or
109 without four hours of warm ambient temperature treatment. *ein2-5* green seedlings
110 subject to four hours of 27°C treatment were used as the negative control. Error bars: \pm
111 S.D., n= 4. Different letters indicate statistical difference in a One-way ANOVA test
112 followed by Tukey's HSD test, $P \leq 0.05$.

113

114
115

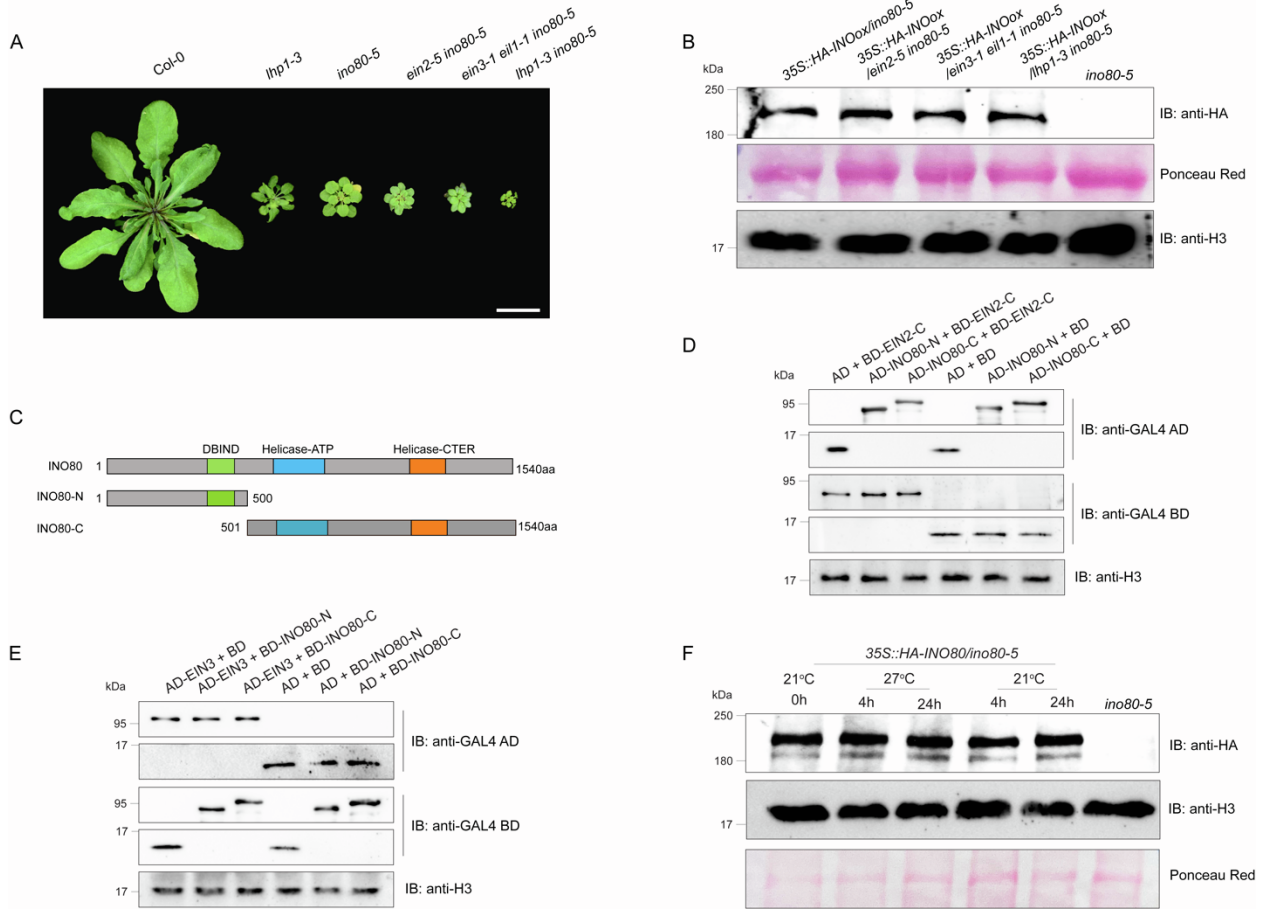
116



118 **Supplemental Figure 5. Supporting Figure 3. Chromatin bivalence of EIN2-LHP1-**
119 **dependent warm ambient temperature induced target genes.**

120 (**A-D**) IGV snapshots of H3K27me3 and H3K4me3 enrichment at *BIM1*, *BUD2*, *GA3ox1*,
121 and *SAUR76* loci. Horizontal black lines represent the amplicons of H3K27me3 and
122 H3K4me3 ChIP-qPCR and P represents ChIP-qPCR primer. (**E**) Heatmap to illustrate the
123 transcriptional response of the subset of warm ambient temperature induced genes (1)
124 whose transcriptional activation depends on both EIN2 and LHP1, (2) bivalently marked
125 by both H3K27me3 and H3K4me3, and (3) with EIN3 binding motifs identified in their
126 promoter regions (Fig. 3C) in Col-0 and in the indicated mutants. Z-score transformed
127 log₂FC value of each gene is plotted in the heatmap. (**F-I**) Sequential ChIP-qPCR of
128 H3K4me3 and H4K27me3 in the indicated plants with or without 4 hours of 27°C
129 treatment. ChIP using IgG was used as a negative control, anti-H3K4me3 was applied for
130 the first ChIP, and anti-H3K4me3 and anti-H3K27me3 were applied for the second round
131 ChIP. Error bars: \pm S.D., n= 4. Different letters were used to indicate the statistical
132 difference between the IP2 H3K27me3/IP1 H3K4me3 (IP2/IP1) ratio values in a One-way
133 ANOVA test followed by Tukey's HSD test, $P \leq 0.05$.

134



135

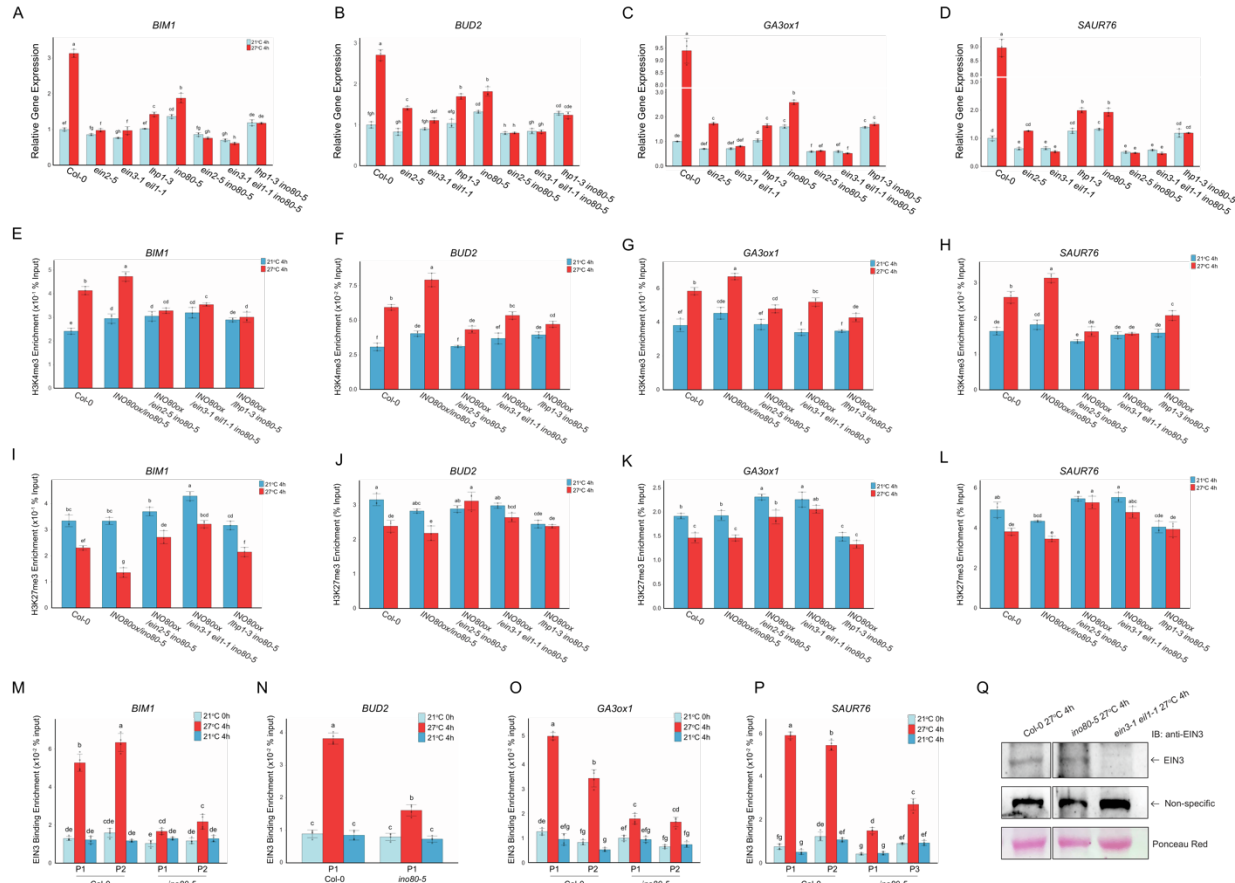
136 **Supplemental Figure 6. Supporting Figure 4. INO80 is genetically associated with**
 137 **EIN2, EIN3, and LHP1.**

138 **(A)** Representative images of six-week-old adult plants of Col-0, *lhp1-3*, *ino80-5*, *ein2-*
 139 *5ino80-5*, *ein3-1eil1-1ino80-5*, and *lhp1-3ino80-5* grown at 21°C in short-day condition.
 140 Scale bar, 2 cm. **(B)** Western blot assay to examine the HA-INO80 fusion protein levels
 141 in complementation transgenic lines of 35S::HA-INO80/*ino80-5*, 35S::HA-INO80/*ein2-5*
 142 *ino80-5*, 35S::HA-INO80/*ein3-1 eil1-1 ino80-5*, and 35S::HA-INO80/*lhp1-3 ino80-5*. Total
 143 protein extracts from five-day-old green seedlings were subjected to anti-HA antibody.
 144 The *ino80-5* mutant seedlings served as negative controls. Ponceau red staining of
 145 Rubisco proteins and anti-Histone H3 were used as the internal loading controls (middle

146 panel and lower panel). **(C)** Diagrams showing the truncation of INO80 to INO80-N (1-
147 500aa) and INO80-C (501-1540aa) used in Figure 4C. **(D-E)** Western blot assays to
148 examine protein expression in yeasts that were used for yeast two hybrid assay as
149 indicated in the figure. Anti-histone H3 was used as a loading control. **(F)** Western blot
150 assay to examine INO80 protein levels under warm ambient temperature condition (27°C).
151 Total protein extracts from five-day-old 35S::HA-INO80/*ino80-5* green seedlings with or
152 without warm ambient temperature treatment were subjected to anti-HA antibody.
153 Ponceau red staining and anti-Histone H3 were used as an internal loading control
154 (middle and lower panel).

155

156



157

158 **Supplemental Figure 7. Supporting Figure 5. EIN2 and EIN3 are required for the**

159 **function of INO80 in warm ambient temperature response.**

160 **(A-D)** qRT-PCR analyses of target gene expressions in *Col-0*, *ein2-5*, *ein3-1 eil1-1*, *lhp1-*
 161 *3*, *ino80-5*, *ein2-5 ino80-5*, *ein3-1 eil1-1 ino80-5*, and *lhp1-3 ino80-5* five-day-old green
 162 seedlings with or without the four hours of 27°C treatment (27°C 4h and 21°C 4h,
 163 respectively). Values are average of relative expression from each gene normalized to
 164 that of *Actin2*. Error bar indicates the SD (n = 4), and different letters indicate statistically
 165 significant differences (One-way ANOVA test followed by Tukey's HSD test, $P \leq 0.05$). **(E-**
 166 **L)** ChIP-qPCR analyses of selected target genes to evaluate the enrichment of H3K4me3
 167 (**E-H**) and H3K27me3 (**I-L**) in *Col-0*, 35S::HA-*INO80/ino80-5*, 35S::HA-*INO80/ein2-5*
 168 *ino80-5*, 35S::HA-*INO80/ein3-1 eil1-1 ino80-5*, and 35S::HA-*INO80/lhp1-3 ino80-5* five-

169 day-old green seedlings treated with 4 hours of 27°C or kept in 21°C for four hours.
170 Individual data point of the methylated H3 enrichment relative to input is plotted as a dot.
171 (**M-P**) ChIP-qPCR analyses of EIN3 enrichment at EIN3 binding motifs in the target genes
172 in Col-0 and *ino80-5*. Values in bar graphs are means ± SD of at least three repeats.
173 Individual data point of the percentage of input is plotted as a dot. For statistical analyses
174 in (**E-P**), significant differences in each group were calculated by using one-way ANOVA
175 with Tukey's test ($P \leq 0.05$) and illustrated by different letters. (**Q**) Western blot assay to
176 examine endogenous EIN3 protein levels in Col-0 and *ino80-5* mutant after four hours of
177 warm ambient temperature treatment (27°C 4h, from ZT4 to ZT8 SD). Total protein
178 extracts from five-day-old green seedlings were subjected to anti-EIN3 antibody. The
179 *ein3-1eil1-1* mutant seedlings served as negative controls. Non-specific bands from the
180 immunoblots (middle panel) and ponceau red staining of Rubisco proteins (lower panel)
181 served as an internal loading control.

182

183

Table S1. Primers used in the study

Primer Name	Sequence	Purpose
LHP1-Y2H-F	ACCGCTCGACAATGAAAGGGCAAGTGGT	Y2H construct
LHP1-Y2H-R	CTAGACTAGTTAAGGCCTCGATTGTACTTG	Y2H construct
INO80-N-Y2H-F	ACCGCTCGACAATGGATCCTCAAGACGACC	Y2H construct
INO80-N-Y2H-R	CTAGACTAGTTATTCTGCCGCTGAAGTTTC	Y2H construct
INO80-C-Y2H-F	ACCGCTCGACAATGCCTCTGAGGTAGAGGATC	Y2H construct
INO80-C-Y2H-R	CTAGACTAGTTAGTTAGCGGAGCTACTTGG	Y2H construct
Ihp1-3-GT-F	CTAACGGGTTCGAGTCTATT	Genotyping
Ihp1-3-GT-R	GCCATTGGGTCTTACATTAT	Genotyping
GST-LHP1-F	CTAGTCTAGACATGAAAGGGCAAGTGGT	Expression vector
GST-LHP1-R	ACCGCTCGACTTAAGGCCTCGATTGTACTTG	Expression vector
GST-INO80-N-F	CTAGTCTAGACATGGATCCTCAAGACGACC	Expression vector
GST-INO80-N-R	ACCGCTCGACTTATTCTGCCGCTGAAGTTTC	Expression vector
LHP1-F	ATTTGGAGAGGACAGGTACCATGAAAGGGCAA GTGGT	Binary vector
LHP1-R	AGTTCTTCGCTCATGTCGACTTGTGTCATCGT CTTTAGTCAGGCCTCGATTGTACTTG	Binary vector
ACTIN2-qRT-F	CCCGCTATGTATGTCGC	Real time PCR
ACTIN2-qRT-R	AAGGTCAAGACGGAGGAT	Real time PCR
BIM1-qRT-F	GCAAGCATCTCCGTTGAAATC	Real time PCR
BIM1-qRT-R	GTCTTGAGCCGTTTGGTTTC	Real time PCR
SAUR76-qRT-F	CTAACCCAGCCACCAGCTCAA	Real time PCR
SAUR76-qRT-R	CTCACGTGGTATGTCCTCCG	Real time PCR
GA3ox1-qRT-F	CCCCAACATCACCTCAACTAC	Real time PCR
GA3ox1-qRT-R	GCTGACCCCAAGTGAATTAG	Real time PCR
BUD2-qRT-F	TCCACGTAACGCCCTGAAGAC	Real time PCR
BUD2-qRT-R	ATCAATGGCCCGGCTTAACA	Real time PCR

BIM1-EIN3-motif-B-P2-ChIP-qPCR-F	CGCTTAGCTCACATGATCAGG	EIN3 binding ChIP qPCR
BIM1-EIN3-motif-B-P2-ChIP-qPCR-R	TGTTCGTACGTGTATGCGTCT	EIN3 binding ChIP qPCR
BIM1-EIN3-motif-A-P1-ChIP-qPCR-F	TGCAGCCAAGCCTAGCTATCAA	EIN3 binding ChIP qPCR
BIM1-EIN3-motif-A-P1-ChIP-qPCR-R	ACGTGGTCTATGTTCGTGTGT	EIN3 binding ChIP qPCR
GA3ox1-EIN3-motif-C-P3-ChIP-qPCR-F	CGATCAATCGTCTACTTGCAGCATATA	EIN3 binding ChIP qPCR
GA3ox1-EIN3-motif-C-P3-ChIP-qPCR-R	ATAAACACACGTGCATTGTTTGATACAC	EIN3 binding ChIP qPCR
GA3ox1-EIN3-motif-B-P2-ChIP-qPCR-F	CCAGATACTGAAAATCTTAGGGAACGTT	EIN3 binding ChIP qPCR
GA3ox1-EIN3-motif-B-P2-ChIP-qPCR-R	GTCCACTAAAGATTAAATTAAATTCAAGATCCATA CA	EIN3 binding ChIP qPCR
GA3ox1-EIN3-motif-A-P1-ChIP-qPCR-F	ACGCCTCTTGCCTAGTATCT	EIN3 binding ChIP qPCR
GA3ox1-EIN3-motif-A-P1-ChIP-qPCR-R	TCGATGACATTGAGTGTGATGAATG	EIN3 binding ChIP qPCR
BUD2-EIN3-motif-B-P2-ChIP-qPCR-F	TGTACACAAGCTTTAGTTAATGTTTAC	EIN3 binding ChIP qPCR
BUD2-EIN3-motif-B-P2-ChIP-qPCR-R	CTATCGCAGGATCGACACTAG	EIN3 binding ChIP qPCR

BUD2-EIN3-motif-A-P1-ChIP-qPCR-F	CAAATCGAACTAACATATCACCTGC	EIN3 binding ChIP qPCR
BUD2-EIN3-motif-A-P1-ChIP-qPCR-R	TGTTCTGTATTCTTGTGTTGTTCTG	EIN3 binding ChIP qPCR
SAUR76-EIN3-motif-C-P3-ChIP-qPCR-F	TCATGAACCTCCTTAGTTGTTGGA	EIN3 binding ChIP qPCR
SAUR76-EIN3-motif-C-P3-ChIP-qPCR-R	ATGGAGTTCCCATTTCCTCGTTT	EIN3 binding ChIP qPCR
SAUR76-EIN3-motif-B-P2-ChIP-qPCR-F	TGATGTATATGGTTGACTGGGATAAC	EIN3 binding ChIP qPCR
SAUR76-EIN3-motif-B-P2-ChIP-qPCR-R	TCGAAAAGATTATGATTATGAATTGGAAAG	EIN3 binding ChIP qPCR
SAUR76-EIN3-motif-A-P1-ChIP-qPCR-F	CTCTCACCGGAAACTCACT	EIN3 binding ChIP qPCR
SAUR76-EIN3-motif-A-P1-ChIP-qPCR-R	TCCTTCGCCATTACCGATTC	EIN3 binding ChIP qPCR
BIM1-ChIP-qPCR-F	GCATTTACTTCGACGCATGATAG	LHP1/H3K4me3/H3K27me3 ChIP qPCR
BIM1-ChIP-qPCR-F	CGACAGCAAATTACGTGAAGC	LHP1/H3K4me3/H3K27me3 ChIP qPCR
GA3ox1-ChIP-qPCR-F	CATTCACCTCCCCACACTCTC	LHP1/H3K4me3/H3K27me3 ChIP qPCR
GA3ox1-ChIP-qPCR-R	TGAGAGGGATGTTTCACCG	LHP1/H3K4me3/H3K27me3 ChIP qPCR
BUD2-ChIP-qPCR-F	AATCCGACCGTTGATCCATC	LHP1/H3K4me3/H3K27me3 ChIP qPCR

BUD2-ChIP-qPCR-R	TTGTGTAAGGGAAAGGCTGAG	LHP1/H3K4me3/H3K27me3 ChIP qPCR
SAUR76-ChIP-qPCR-F	TCAACACCAAGCCTAACAG	LHP1/H3K4me3/H3K27me3 ChIP qPCR
SAUR76-ChIP-qPCR-R	GGAGCTCACGTGGTATGTC	LHP1/H3K4me3/H3K27me3 ChIP qPCR

186

187
188**Table S2. Summary of total clean reads and aligned reads**

mRNA sample name	Clean reads	Aligned reads	mapping rate (%)
Col-0 21°C rep 1	47865865	32881507	68.70
Col-0 21°C rep 2	63670616	43087184	67.67
Col-0 27°C rep 1	48137932	36701642	76.24
Col-0 27°C rep 2	38190854	30216474	79.12
<i>ein2-5</i> 21°C rep 1	40708589	31212208	76.67
<i>ein2-5</i> 21°C rep 2	39604543	29856840	75.39
<i>ein2-5</i> 27°C rep 1	35391014	26788765	75.69
<i>ein2-5</i> 27°C rep 2	46371399	36137094	77.93
<i>ein3-1 eil1-1</i> 21°C rep 1	40989763	24153109	58.92
<i>ein3-1 eil1-1</i> 21°C rep 2	82799179	47566071	57.45
<i>ein3-1 eil1-1</i> 27°C rep 1	50658266	38080160	75.17
<i>ein3-1 eil1-1</i> 27°C rep 2	45220023	33483559	74.05
<i>lhp1-3</i> 21°C rep 1	64463244	41153114	63.84
<i>lhp1-3</i> 21°C rep 2	49571904	30804712	62.14
<i>lhp1-3</i> 27°C rep 1	58246905	42625800	73.18
<i>lhp1-3</i> 27°C rep 2	40045071	27865315	69.58
<i>ein2-5 lhp1-3</i> 21°C rep 1	47443065	31419916	66.23
<i>ein2-5 lhp1-3</i> 21°C rep 2	53528785	33209942	62.04
<i>ein2-5 lhp1-3</i> 27°C rep 1	40516538	24445082	60.33
<i>ein2-5 lhp1-3</i> 27°C rep 2	53247799	32048866	60.19

189
190